Diverse yet highly selective interorgan crosstalk mechanisms shape the bodywide transcriptome landscape

Norio Takada[1, 2, *], Madoka Omae[1, 3, *], Fumihiko Sagawa[1, 2], Neil C. Chi[4], Satsuki Endo[1, 2], Satoshi Kozawa[1, 2], Thomas N. Sato[1, 2, 5, 6, ¶]

The Thomas N. Sato BioMEC-X Laboratories, Advanced Telecommunications Research Institute International (ATR), Kyoto, Japan[1]; ERATO Sato Live Bio-Forecasting Project, Japan Science and Technology Agency (JST), Kyoto, Japan[2]; Kyoto University, Graduate School of Biostudies, Kyoto, Japan[3]; Division of Cardiovascular Medicine, Department of Medicine, University of California, San Diego, La Jolla, CA, USA[4]; Department of Biomedical Engineering, Cornell University, Ithaca, NY, USA[5]; Centenary Institute, Sydney, Australia[6]

*These two authors contributed equally to this work

[¶]Corresponding Author:

Thomas N. Sato

The Thomas N. Sato BioMEC-X Laboratories

Advanced Telecommunications Research Institute International (ATR)

2-2-2 Hikaridai, Seika-cho, Soraku-gun, Kyoto, Japan 619-0288

Email: island1005@gmail.com

TEL: 81-774-95-2311

FAX: 81-774-95-2329

SUMMARY

The network of functionally diverse organs is vital for organismal development and function. Despite such importance, the knowledge of the bodywide interorgan communication network is severely limited. Hence, we generate comprehensive bodywide transcriptome datasets following the systematic organ-ablations and organ-specific gene mutations in zebrafish and the data are integrated into a mechanistic interorgan network model. The experimental validation of the model unveils unexpectedly more diverse and selective interorgan crosstalk mechanisms than conventionally assumed to orchestrate the expression of 73 genes implicated for differential organ development and function across 8 organs. The findings provide an important insight into how differential organ development and function may be regulated at the organismal level by the cardiovascular system, which is a primary mediator of the interogan crosstalk in all vertebrates. Furthermore, the panoramic bodywide landscape shown herein and available at i-organs.atr.jp serves as a platform resource for studying organ-to-organ interactions at the organismal level.

INTRODUCTION

The organ-to-organ crosstalk is critical for development and physiological homeostasis (Droujinine and Perrimon, 2013). Failure or dysfunction of such interorgan communication system severely hampers the development and functions of virtually all organs (Droujinine and Perrimon, 2013; Noble, 2002; Rajan and Perrimon, 2011; Stainier, 2001). Despite such importance, a comprehensive understanding of the interorgan signaling mechanism regulating the diverse organ functions is lacking.

Each organ may discriminate among the various interorgan signals. In addition, the differential combination of interorgan signals may be delivered to each organ via differential mechanisms. The molecular and cellular underpinnings of such bodywide organ-to-organ interactions are important but defining them remains challenging. Furthermore, only a small subset of interorgan interactions are currently known and the bodywide landscape of such interactions are lacking.

This is, in part, due to the fact that such problems have been traditionally studied based on the previous knowledge about the interorgan crosstalks. In contrast, a bodywide and unbiased approach may provide an advantage and that comprehensive bodywide profiles representing the molecular-level changes in each organ resulting from the specific ablation and/or mutations of the interorgan crosstalk signals would be extremely useful. However, this approach is intractable, in particular for vertebrate models with closed circulatory systems, as organs do not form in the absence of the cardiovascular system, a primary mediator of the interorgan communication.

One exception is zebrafish (Stainier, 2001; Weinstein and Fishman, 1996). While zebrafish possess a closed circulatory system, organ-formation appears to initiate and proceed at least to a certain extent even in the absence of the cardiovascular system (Liao et al., 1997; Stainier, 2001; Weinstein and Fishman, 1996). Hence, zebrafish provide a model vertebrate system for

such an analysis. Zebrafish also provide a relatively simple vertebrate model system where genetic tools are already available for organ-specific ablations and systematic mutations of organ-specific genes (Stainier, 2001; Weinstein, 2002).

Here, we used this vertebrate model organism to generate and characterize the dynamic changes of the comprehensive bodywide transcriptome landscapes upon the ablations of the heart and the vasculature, two primary components of the cardiovascular system, and also the liver, the largest organ regulating bodywide metabolism. We also characterized the bodywide transcriptome landscapes of the mutants for 3 cardiac-specific genes, each of which exhibit differential contractile phenotype. Additionally, the effects of the mutations of 9 liver- and liver/kidney specific genes were individually characterized. These datasets were integrated into a mechanistic model describing how differential interorgan crosstalk mechanisms could regulate the distinct functions of each organ and also the distinct processes within the same organ. The experimental validation of the model unveiled unexpectedly diverse yet selective interorgan crosstalk mechanisms that differentially regulate 73 genes implicated to support and/or guide the differential organ development and function across 8 organs. The findings are summarized as a bodywide landscape depicting the interorgan genetic interaction network that serves as a platform resource for studying organ-to-organ interactions at the organismal level. This landscape is also made available at i-organ.atr.jp as a public resource.

RESULTS

"Heartless" and cardiac-specific gene mutants

The bodywide comprehensive transcriptome analysis was performed on "heartless" zebrafish larvae. The "heartless" was generated by treating *Tg*(*cmlc2:mcherry-NTR*) zebrafish larvae with MTZ (Curado et al., 2007; Curado et al., 2008; Dickover et al., 2013) (Fig. 1a, see METHODS). The specific ablation of cardiac muscle, but not endocardium/endothelial cells, was confirmed by the lack of cardiac muscle fluorescent reporter expression (Fig. 1a), and the presence of

endothelial reporter gene expression, *fli1a:efgp*(Isogai et al., 2003; Lawson and Weinstein, 2002) (Fig. 1a). The "heartless" larvae at 4.5 dpf (days post fertilization) were processed for genome-wide transcriptome analysis.

The wholebody RNAseq analyses followed by the Gene Ontology (GO) enrichment analysis found differentially regulated genes including those related to stimulus via external cues, stress, immune responses, and homeostasis (Fig. 1b, raw data available at i-organs.atr.jp). The RNAseq data, followed by the qRT-PCR validation, confirmed the significant reductions in known cardiomyocyte-specific genes (myl7, cmlc1, tnnc1a, nppa, etc.) (Fig. 1c, Table S1), further validating the cardiomyocyte-specific ablation. The analysis identified 54 genes whose expression levels were reproducibly altered in non-cardiac organs in "heartless" larva (Fig. 1c, Table S1). Wholemount in situ hybridization (WISH) analyses identified their expression patterns: 22 specifically in the liver, 3 in the liver and the kidney, 1 in the somite, 1 in the pancreas, 1 in the liver and the somite, 2 in the liver and undefined tissues, 1 in the somite and undefined tissues, 23 in unidentified or undetermined tissues (Figures S1&S2, Table S2), each representing mostly organ-specific gene implicated for the organ-specific physiological functions such as fatty-acid metabolism for the liver, transporters and enzymes for the kidney, a hormone for the pancreas, etc.. Many of the 23 genes found to be upregulated in unidentified or undetermined tissues encode proteins involved in immune responses, inflammation and/or tissue remodeling. The liver-specific expression was also confirmed by transcriptome analysis of the liver-specific ablation line (Curado et al., 2007; Curado et al., 2008) and also of the isolated liver tissue (see METHODS, Figure S3, Table S1).

Next, we determined whether a single cardiomyocyte-specific gene mutation is sufficient to induce the same effects as in "heartless". Three genes encoding contractile cardiac-muscle-specific proteins were individually mutated (Fig. 1d). Mutations were introduced into myl7, cmlc1 and tnnc1a genes by the CRISPR/Cas9 system (Gagnon et al., 2014; Jao et al., 2013; Thomas et al., 2014) (see METHODS, Figure S4a, b). Both myl7 and

cmlc1 mutations resulted in the indistinguishable contractile dysfunction of the heart (Movies S1 – S3). The tnnc1a mutation resulted in the lack of ventricular, but not atrial, contraction (Movie S4), correlating with its ventricular-specific expression. No circulation was observed in any of these three mutants (Movies S5 – S7).

The qRT-PCR analysis of the 54 non-cardiac genes differentially regulated in "heartless", 4 cardiac genes (myl7, cmlc1, tnnc1a and nppa), and 6 liver genes that are unaffected in "heartless" was performed in each mutant (Fig. 1d, Table S1). The results with the cardiac gene mutants unveil the common and distinct cardiac properties differentially regulating the gene expressions in each non-cardiac organ (Fig. 1e): (I) Positive regulation by any one of the three cardiac-genes; (II) Positive regulation by the myl7 mutant, but not by cmlc1 or tnnc1a; (III) Positive regulation by myl7 and tnnc1a, but not by cmlc1; (IV) Negative regulation by all three cardiac genes; (V) Negative regulation by cmlc1 and tnnc1a, but not by myl7; (VI) Negative regulation by tnnc1a, but not by myl7 or the cmlc1.

The differential effects of the mutations on another cardiomyocyte-specific gene, nppa, suggest the genetic interactions among the cardiac-genes (Fig. 1e). In the myl7 mutant, the cmlc1 and tnnc1a expressions were partially reduced. In contrast, in both cmlc1 and tnnc1a mutants, the myl7 expression is not affected, despite the nppa upregulation. These results suggest that the nppa expression is under the negative regulations of both cmlc1 and tnnc1a. Moreover, both cmlc1 and tnnc1a appear to be under the regulation of yet another identified input pathway(s), as nppa expression is unaffected by the myl7 mutation which partially reduces the cmlc1 and tnnc1a expression (Fig. 1e).

The gene expression effects induced the myl7 mutation were completely rescued (R^2=0.95501) by the re-expression of myl7 using the myl7 cardiomyocyte-specific promoter (Figure S4c, d; Table S1), which was accompanied by the complete rescue of contractile and circulatory dysfunctions (Movie S5). This result supports the idea that the effects of myl7 mutation are due to its functions in cardiomyocytes. The re-introduction of cmlc1 using the

myl7 promoter (Figure S4c, Table S1) rescued the cardiac contractility, but not the circulation (Movie S6). The gene expression effects were partially rescued (R^2=0.76025) (Figure S4d, Table S1), suggesting that cardiac contraction alone is mostly sufficient to rescue the normal gene expression pattern in the cmlc1 mutant. In contrast, the re-expression of tnnc1a under the control of the myl7 promoter failed to rescue the cardiac functions or the gene expression pattern (Movie S7, Figure S4d, Table S1). This is presumably due to the fact that tnnc1a is expressed in ventricle, but not in atrium, and the transgene tnnc1a under the control of the myl7 promoter is expressed in both ventricle and atrium, resulting in aberrant contractions (Movie S7). The results suggest that the aberrant contraction is not sufficient for the normal gene expression pattern – "the normal" contraction is required.

Liver gene mutants

Many genes influenced in "heartless" are liver-genes (Fig. 1e). Hence, a possibility of their cross-regulation was examined by analyzing the mutants for 11 liver genes (Figure S5a, b). The expression of the 54 genes regulated in "heartless" was mostly unaffected in any of these mutants (Fig. 2a, Table S1). Only subtle, but statistically significant, influences were detected with a few genes in two mutants: sepp1b and lepa in cbln13 mutant, cbln9 in rpb2b mutant, indicating the presence of only a weak cross-regulations among them (Fig 2a, Table S1). There are other genes that are weakly influenced such as scpp8 in cbln13 mutant, and itln3 in fabp10a mutant (Fig. 2a). The expression of these genes was, however, upregulated in "heartless," while in each mutant their expression is downregulated. Such influences in the opposite directions in "heartless" and the mutant are inconsistent with the possibility of a cross-regulation among these genes.

Since only weak cross-regulations among the liver genes were found at 4.5 dpf, the gene expression was studied in these mutants at later stages where the interorgan crosstalk is presumably more complex. Comprehensive transcriptome analyses were performed using 30

dpf juveniles of the liver-gene mutants (Figure S5a, b). One such candidate gene, bscl2l, was found whose expression was dependent on dpys, a gene expressed in both the liver and the kidney. In the dpys mutant, the bscl2l expression remains unchanged at 4.5 dpf or 10 dpf, but is significantly reduced at 30 dpf (Fig. 2b, Table S1). To identify the organs where bscl2l is expressed and where its expression is affected by the dpys mutation, several organs of 30 dpf juvenile fish were isolated (Figure S5c, Table S1) and the level of bscl2l in each organ was measured by qRT-PCR. Expression of bscl2l was detected in several organs with the highest level in the pancreas (Figure S5d, Table S1). The largest reduction was, however, found in the intestine (Fig. 2c, Table S1). The results using the liver gene mutations are summarized in Fig. 2d, illustrating the weak cross-regulations among liver genes and stronger interaction between liver/kidney (dpys) and non-liver gene (bscl2l) (Fig. 2d).

"Vesselless"

The bodywide transcriptome landscape in the absence of the vascular network was studied using *cloche* (Liao et al., 1997; Reischauer et al., 2016) (referred to as "vesselless" here) (Fig. 3a). The absence of the vessels and endocardium, but the presence of cardiac muscle and contraction was confirmed (Fig. 3a, Movie S8). The comprehensive transcriptome analysis of "vesselless" larva at 5 dpf revealed many vascular and non-vascular genes whose expression was differentially affected. GO enrichment analysis using the RNAseq datasets (available at i-organs.atr.jp) found both commonly and distinctly enriched GO terms between "vesselless" and "heartless" (Fig. 3b). Many of the GO terms enriched for "heartless" are also enriched for "vesselless (Fig. 3b). In addition, there are a number of GO terms that are specifically-enriched for "vesselless" (Fig. 3b.). The most prominent of these "vesselless"-specific terms are those related to sensory system and cell-cell signaling (Fig. 3b). Validation studies by qRT-PCR identified 13 non-vascular genes whose expression was significantly and reproducibly altered in "vesselless", but not or only weakly altered in "heartless" (Fig. 3c, Table S1). Four (ompa,

pglyrp2, crx, rx1) were downregulated and nine (hmgcra, sqlea, lss, nsdhl, ebp, cyp51, memo1, scd, fads2) were upregulated (Fig. 3c). All of the upregulated genes encode enzymes critically involved in cholesterol biosynthesis (Lu et al., 2015; Mazein et al., 2013; Paton and Ntambi, 2009) (Figure S6). WISH analyses indicated that all were expressed in the liver, and five (hmgcra, sqlea, lss, msmo1, fads2) were also expressed in the brain and two (hmgcra, fads2) in the intestine (Fig. 3d). Two downregulated genes, crx and rx1, are eye-genes, confirming the previous report (Dhakal et al., 2015). One newly identified downregulated gene, ompa, is expressed in the olfactory bulb (Fig. 3e). The comparison to WISH patterns of a pan-olfactory-bulb marker, ompb(Celik et al., 2002), shows that both ompa and ompb are expressed in the olfactory bulb, but the ompa expression is restricted to a subset of neuroepithelial cells of the bulb (Fig. 3e). Only weak signals were detected for another olfactory bulb-specific gene, ora1(Ahuja and Korsching, 2014; Behrens et al., 2014), in wild type and in "vesselless" (Fig. 3e, Table S1). Another newly identified downregulated gene, pglyrp2, a cellular protein known for its important role in innate immune response, was expressed in the liver and multiple other undefined organs/tissues (Figure S2c). That such differential expressions of the genes were due to the lack of the vessels is further supported by the characterization of etv2 morphant (Figure S7). Etv2 morpholino injection was previously shown to reduce the vascular network in a relatively specific manner (Craig et al., 2015; Sumanas and Lin, 2006; Veldman and Lin, 2012) (Figure S6a). Gene expression correlation analysis between "vesselless" and etv2 morphant showed a high correlation coefficient (R^2=0.81821) (Fig. 3f, Table S1), supporting the idea that the differential gene expressions in "vesselless" is likely due to the lack of vessels, rather than the direct effects of the cloche gene mutation. The results of "vesselless" are summarized in Fig. 3g.

Modeling and experimental validation of diverse interorgan mechanisms

The findings hitherto suggest the cardiomyocytes, distinct cardiac contraction properties and the

vessels impose differential influences on the bodywide transcriptome landscape (Figs. 1e & 3g). To integrate such findings and gain a mechanistic insight, we developed a model describing how the differential gene expression in each organ could be regulated (Fig. 4a). Four distinct mechanisms could be formulated: (M1) Cardiomyocytes and/or cardiac contraction deliver systemic factors via vessels to regulate the gene expression in a non-cardiac organ; (M2) Upon cardiac dysfunction and/or in the absence of cardiomyocytes, systemic factors are induced and delivered to non-cardiac organ to regulate the gene expression there; (M3) Cardiomyocytes and/or cardiac contraction provide non-systemic factors via a non-vascular mechanism to regulate the gene expression in a non-cardiac organ; (M4) Vessels locally regulate the gene expression in a non-cardiac organ in a cardiac-independent manner. A, C, E and G are groups of genes positively regulated by M1, M2, M3 and M4 mechanisms, respectively. B, D, F and H are groups of genes negatively regulated by M1, M2, M3 and M4 mechanisms, respectively. Fig. 4a describes how each gene behaves in "heartless", "vesselless", and the combination of both. A simulation (Fig. 4b, left panel, Figure S8) predicted the qRT-PCR results for each category of the genes (Fig. 4b, right panel). The actual experimental results are shown as a heatmap in Fig. 4c (also Table S1). Based on these results, each gene is classified to a specific group (A – H) and summarized in Fig. 4d.

All findings in this paper are summarized in Fig. 5, depicting how the expression of each gene in each organ is regulated by distinct and/or common interorgan mechanisms mediated by the cardiovascular system. In the liver and kidney, more genes (13 genes) are under the distantly-acting positive regulations (A, D, E categories) of the cardiovascular system. Such regulation is differentially mediated by cardiac genes (myl7, cmlc1, tnnc1a) or the contraction properties (I, II, III, IV, V) (Figs. 1e&5). In contrast, the genes expressed in less discrete organs/tissues (i.e., "others") are under the distantly-acting negative regulation (B, C, F categories), and they are all negatively-controlled by all these (myl7, cmlc1, tnnc1a) cardiac-genes or contraction (IV). One exception is the mmp13a expression which is mediated

specifically by the tnnc1a function (VI). No genes in these tissues/organs appear to be under distantly-acting positive regulation (A, D, E categories). Other organ specific responses can be found in sensory organs. In the olfactory bulb and eye, the cardiovascular system appears to locally-act on subsets of neuroepithelial cells in the positive direction (G category) (Figs. 4&5). In the olfactory bulb, ompa is under the positive regulation of the vascular endothelial cells. In the eye, crx and rx1 also are regulated by the same mechanism (Fig. 3g). This regulatory mode could not be found in other organs, except for pglyrp2 gene which was expressed in the liver and other tissues (Fig. 5).

DISCUSSION

In the classic view, the heart generates force to deliver systemic factors such as oxygen, nutrients, hormones, etc. to distant organs via vessels to maintain homeostasis of the body(Aaronson et al., 2014; Noble, 2002). In addition, the immune cells reach to the distant organs via vessels upon inflammation (Aaronson et al., 2014; Noble, 2002). M1 (A, B) and M2 (C, D) (Figs. 4a) correspond to these classic cardiovascular mechanisms, respectively. This study unveils an unconventional mechanism, M3 (E, F), where a cardiac-derived mediator acts on distant organ(s) independently of the vessel circulation. What could be the mediator(s)? The possibility of the neural system involvement was examined. We tested this possibility by specifically ablating a subset of dopaminergic (DA) neurons, a neural type that is known to be involved in a number of homeostatic processes including the regulation of cardiovascular functions (Aaronson et al., 2014; Myers and Olson, 2012; Noble, 2002). A subset of DA neurons was genetically ablated by the double mutations of otpa and otpb genes(Fernandes et al., 2013) (Figure S9a). The expression of the genes that belong to M3 (E, F) was quantitatively analyzed by qRT-PCR (Figure S9b, Table S1). While the ablation of these DA neurons was confirmed by the downregulation of oxt as previously described (Fernandes et al., 2013), none of the genes in E or F categories exhibit the regulated expressions that are consistent with the

possibility of otpa/otpb-positive DA neurons as the mediators (Fig. 9b). The expressions of il4r.1 and timp2b are slightly downregulated in the otpa/otpb double mutant, but the direction of the effects is opposite. Hence, it is unlikely that DA neurons mediate the cardiovascular effects on these genes in distant organs. What are then the mediators? Diffusible cardiomyocyte-derived factors? The identification of such cardiomyocyte-derived mediator(s) may provide an important step towards a more complete understanding of the cardiovascular mechanisms that influence the organ development and functions.

We also identified a vessel-dependent, but independent of cardiomyocytes or the circulation, mechanism (M4: G, H). The expressions of ompa and pglyrp2 were found to be dependent on the presence of vessels (Figs. 3a&5). The ompa expression was detected in a specific subset of the olfactory neural epithelial cells (Fig. 3e). The pglyrp2 expression appears to be in multiple tissues/organs including the liver (Figure S2c). While the critical roles of the vessels in the development of the liver and the pancreas have previously been shown(Lammert et al., 2001; Matsumoto et al., 2001), the question of whether such local effects are independent of the circulatory force remained controversial. The present study shows that the circulation-independent local-vessel-mediated mechanism, at least in part, contributes to the ompa and pglyrp2 expression. Further, neurovascular interactions are critical in development and disease(Weinstein, 2005). The data show that the local vessel-mediated expressions of ompa & crx/rx1 in the olfactory bulb and the eye, respectively. Hence, it is possible that these neural tissues are more susceptible to the local presence of the vessels.

The expression of the genes encoding enzymes for cholesterol biosynthesis is also under the negative local regulation by the vessels (Figs. 3g & 5). Cholesterol in the circulation is taken up by the vascular endothelial cells via endocytosis (Anderson et al., 2011; Ho et al., 2004). This endothelial mechanism is critical to maintain the homeostasis of cholesterol level in the circulation (Anderson et al., 2011; Ho et al., 2004). It is possible that such a mechanism operates as a negative feedback, suppressing the expression of the genes encoding enzymes for

cholesterol biosynthesis – hence, the absence of the vessels results in the upregulation of these genes. The treatment of the wild type or "heartless" zebrafish larvae by atorvastatin (D'Amico et al., 2007; Mathews et al., 2014) resulted in the upregulation of these genes (Figure S10, Table S1). The atorvastatin treatment of "vesselless" resulted in only a weak or no upregulation of expression of these genes (Figure S10, Table S1), supporting the notion that the expressions of these genes are in a negative feedback loop where the vascular endothelial cells function as a suppressive interface in an circulation-independent manner.

In conclusion, the present study provides a genome-wide and whole-body level profiles unveiling the unexpected divergence and coherence in the interorgan communication mechanism regulating the gene expression in various organs. The findings provide an insight into how differential organ development and function may be regulated at the organismal level by the cardiovascular system, a primary mediator of the interorgan crosstalk. The bodywide interorgan transcriptome landscape shown here also serves as a platform resource for studying organ-to-organ interactions at the organismal level. The expression of the genes shown in Fig. 5 could also serve as organ-specific functional reporters for the functional states of the cardiovascular system for the studies of vertebrate development. Many diseases are caused by the changes of the functional states of the cardiovascular system (Noble, 2002). Hence, it is possible that the altered gene expression shown in this paper could be exploited to evaluate the effects of a therapeutic treatment on such diseases.

METHODS

Fish husbandry

Zebrafish were maintained in circulation-type aquarium system (Iwaki) with 14 h/day and 10 h/night cycle at around 27^{o}C. The fertilized eggs were collected and raised at 28.5^{o}C in egg water (0.06% artificial marine salt supplemented with 0.0002% methylene blue) until around epiboly stage and subsequently in 1/3 Ringer's medium (1.67 mM HEPES, 38.7 mM NaCl, 0.97

mM KCl, 0.6 mM $CaCl_2$, pH 7.2) containing 0.001% phenylthiourea (PTU) (Sigma) to prevent pigmentation. Embryos and larvae were staged to days post fertilization (dpf) according to Kimmel *et al* (Kimmel et al., 1995). Zebrafish maintenance and experiments were conducted in accordance with animal protocols approved by the Animal Care and Use Committee of Advanced Telecommunications Research Institute International (A1403, A1503, A1603).

Transgenic reporter fish

The following zebrafish lines were used: *Tg(cmlc2:mcherry-NTR)*(Dickover et al., 2013), *Tg(fabp10a:CFP-NTR)* (Curado et al., 2007; Curado et al., 2008), *Tg(lfabf:DsRed; elaA:egfp)* (Korzh et al., 2008), *Tg(fli1a:egfp)*^{y1}(Lawson and Weinstein, 2002) and *Tg(gata1:DsRed)* (Traver et al., 2003).

Cardiomyocyte / liver ablation

The cardiomyocyte-specific ablation was performed by treating *Tg(cmlc2:mcherry-NTR)* by Metronidazole (MTZ). *Tg(cmlc2:mcherry-NTR)* heterozygous fish were crossed with wild-type to obtain *Tg(cmlc2:mcherry-NTR)*$^{+/Tg}$ eggs. Eggs were raised at 28.5^{o}C in egg water to around epiboly stage and subsequently in 1/3 Ringer's medium containing 0.001% PTU to prevent pigmentation. At 2 - 3 dpf, embryos were sorted by mcherry fluorescence under Leica M165 FC microscope (Leica). At 3 dpf, the embryos were treated either with 0.2% DMSO alone and 10 mM MTZ with 0.2% DMSO in 1/3 Ringer's media containing 0.001% PTU for 6 hrs, followed by washing with 1/3 Ringer's medium 3 times for 5 min each. After the washing, embryos were again raised in 1/3 Ringer's medium containing 0.001% PTU for 20 hrs at 28.5^{o}C.

For the liver-specific ablation, *Tg(fabp10a:CFP-NTR)* homozygous fish were used. *Tg (fabp10a:CFP-NTR)* embryos/larvae were treated with 7 mM MTZ prepared as above from 2.5 dpf to 5.5 dpf. MTZ-containing media was changed everyday during the treatment.

Cloche mutant

Cloche^{la1164}*(clo*^{la1164}*)* (Liao et al., 1997; Reischauer et al., 2016) (provided by Dr. Kawakami) was maintained by mating with wild-type fish. Genotyping of *clo*$^{la1164/la1164}$ was conducted by observing the heart morphology and the absence of the circulation of embryo. C*lo*$^{+/la1164}$ was crossed with *Tg(cmlc2:mcherry-NTR)*$^{+/Tg}$ and *Tg(fli1a:egfp)*$^{+/y}$ to generate double heterozygous fish of *clo*^{la1164} *allele* and a reporter gene allele. To genetically ablate the cardiomyocyte in *clo*$^{la1164/la1164}$ embryo, *clo*$^{+/la1164}$ was mated with *clo*$^{+/la1164}$*;Tg(cmlc2:mcherry-NTR)*$^{+/Tg}$. At 3 dpf, *clo*$^{+/?}$*;Tg(cmlc2:mcherry-NTR)*$^{+/Tg}$ and *clo* $^{la1164/la1164}$*;Tg(cmlc2:mcherry-NTR)*$^{+/Tg}$ were treated with 0.2% DMSO and 10 mM MTZ in 1/3 Ringer's medium with 0.001% PTU/0.2% DMSO for 11 hrs. After washing out the solution, the embryos were raised as described in the cardiomyocyte-ablation section.

Organ dissection

A liver was dissected out from a larva at 4.5 dpf under stereotype fluorescent microscope. To isolate a liver free of other organs/tissues, we used *Tg(lfabf:DsRed;elaA:egfp)* that labels hepatocytes with DsRed fluorescence. The dissected liver and remaining body were placed in a 1.5 ml tube and quickly frozen on dry ice.

After fasting for one day juvenile zebrafish at 30 dpf were anesthetized and the heart, the liver, the intestine, the kidney and the pancreas were dissected and isolated under the stereomicroscope. The organs and remaining body were placed in a 1.5 ml tube and then quickly frozen on liquid nitrogen.

RNA extraction

To obtain total RNA, embryos and larvae were harvested in a 1.5 - 2 ml tube at appropriate stage and frozen in liquid N_2 to be stored in -80^{o}C. To prepare total RNA for RNAseq analysis of embryonic and larval stages, 10 - 20 embryos and larvae were pooled in a 1.5 ml tube, and

total RNA was isolated using RNeasy Mini Kit (QIAGEN). The pooled embryos/larvae were homogenized in Buffer RLT included in the kit using 5 ml syringe and 24G needle by passing through the needle for 20 times. After homogenization, the manufacture instruction was followed. To prepare RNA for real-time PCR analysis, embryos/larvae were individually harvested in a 1.5 ml or 2 ml tube and total RNA from each individual embryo/larva was isolated by AllPrep DNA/RNA Mini kit (QIAGEN). Individual Embryo/larva was either homogenized using a syringe as described above or crashed in 700 μl Buffer RLT using approximately 50 zirconia balls with 1.5 mm diameter (YTZ balls) (NIKKATO) by centrifuging at 4260 rpm for 60 sec in Cell Destroyer PS1000 (BMS). After the homogenization or crushing, the manufacture instructions were followed. Subsequently, the isolated genomic DNA and total RNA were subjected to genotyping and reverse transcription reaction.

RNA sequencing

Total RNA was prepared from two biological replicate pools of 4.5 dpf wild type and cardiomyocyte-ablated larvae and 5.5 dpf wild type, cloche mutant and the liver-ablated larvae. Each pool had about 15 larvae. Total RNA of 10 dpf and 30 dpf zebrafish was prepared by mixing equal amount of total RNA isolated from 5 - 10 single zebrafish prior to the RNA quality check by Agilent 2100 Bioanalyzer (Agilent, CA, USA). The RNAseq analysis (read length:100 bp, total reads number per sample: about 100 million, single-end read) for Fig. 1 and Figure S3 was performed using Illumina HiSeq 2500. RNAseq analysis (read length: 100 bp, total reads number per sample: about 100 million, pair-ends read) for 30 dpf juveniles of cbln13, dpys, fabp10a, tgm2a and uox mutants was performed with Illumina HiSeq 2000/TruSeq RNA Sample Prep Kit (Illumina). The data were mapped to the zebrafish genome (Zv9) with Bowtie2(Langmead and Salzberg, 2012; Nellore et al., 2016) running on Galaxy (https://usegalaxy.org/) (Afgan et al., 2016). The obtained bam file was used to calculate fragments-per-kilobase-of-exon-per-million (FPKM) of transcripts and the differential gene

expression data using Cuffdiff (Trapnell et al., 2010). To perform Gene ontology enrichment analysis, the enriched genes were defined as an absolute of log_2fold-changes is greater than or equal to 1 and p-value is less than 0.05. A gene ontology enrichment analysis is performed by R package "topGO" using a root category "BP" and a reference database "org.Dr.eg.db". To prepare volcano plot graph from RNAseq data, p-value and fold-change was calculated using DESeq2 (Love et al., 2014) with default settings.

Quantitative RT-PCR (qRT-PCR) analysis

Total RNA (30 - 150 ng) was used to perform reverse transcription using SuperscriptIII reverse transcriptase primed with oligo(dT) (Invitrogen). After the reaction, the mixture was diluted to 1:3 - 1:10 to prepare a working solution. Real-time qPCR was performed using LightCycler 480 SYBR Green Master (Roche) in combination with LightCycler 480 machine (Roche). The final reaction mixture (10 µl volume) was prepared as followings: 5 µl of LightCycler 480 SYBR Green I Master, 2 µl of RNase-free water, 0.5 µl of 10 µM forward primer, 0.5 µl of 10 µM reverse primer, 2 µl of cDNA template. The mixture was dispensed using epMotion P5073 automated pipetting system (Eppendorf). All qPCR was performed using 384 white-plate PCR platform. PCR cycle was as followings: 10 minutes at 95 ^{o}C, 45 cycles of 10 sec. 95^{o}C, 10 sec. at 63^{o}C, 10 sec at 72^{o}C. Amplification and dissociation curves were generated by the LightCycler 480 Software (release 1.5.1.62 SP2). Primers used for qPCR were designed using the Roche Universal ProbeLibrary Assay Design Center (https://qpcr.probefinder.com/organism.jsp). The primer sequences were listed in supplementary information 1. The transcript levels of measured genes were normalized with *rpl13a* level for all experiments except for the data of Fig. 2.

Whole-mount in situ hybridization (WISH)

To synthesize an antisense RNA probe, the template DNA was amplified by PCR using

KOD-Plus-Neo (TOYOBO) from cDNA synthesized from zebrafish total RNA of appropriate stage of WT or cloche mutant (for hmgcra, sqlea, nsdhl, cbp, fads2). For ora1, lss, cyp51, msmo1, scd, ompa and ompb, the cDNA sequences were chemically synthesized for use as templates of PCR. The primers used for PCR are listed in Supplementary Table 2. Primer sequence was designed using Blast primer (NCBI/ Primer-BLAST: http://www.ncbi.nlm.nih.gov/tools/primer-blast/) and, T3 and T7 sequence were added at 5' end of forward and reverse primer, respectively. PCR product was purified by QIAquick PCR Purification Kit (Qiagen). The sequence was confirmed by reading it using T3 and T7 primer. For synthesizing antisense RNA probe, the following mixture was used: DIG RNA labeling mix (Roche Diagnostics), Transcription buffer (Roche Diagnostics), RNase inhibitor (Roche Diagnostics), T7 RNA polymerase (Roche Diagnostics), and 200 ng of template DNA. Then it was incubated for 1.5 - 3 hour at 37^{o}C, followed by precipitation with lithium-chloride precipitation solution. Precipitated DIG-labeled RNA was re-suspended in nuclease free water and mixed with equal volume of formamide to be stored at -80^{o}C.

To prepare embryos for whole mount in situ hybridization, anesthetized zebrafish embryos/larvae were fixed in 4% Paraformaldehyde Phosphate Buffer Solution (PFA) (Nacalai Tesque) overnight at 4^{o}C. The fixed embryos were dehydrated three times for 5 minutes in 100% methanol at room temperature and were stored at -30^{o}C for at least 2 days. Before hybridization, the embryos in methanol were dehydrated five times for 5 minutes in PBST (phosphate buffered saline containing 0.1% Tween-20), and then permeabilized in 10 µg/ml proteinase K in PBST for 30 minutes at room temperature. After quick wash with PBST, the embryos were post-fixed for 20 minutes in 4% PFA at room temperature, and then washed 5 x 5 minutes in PBST. Then, the embryos were incubated in hybridization solution (50% formamide, 5×SSC, 50 µg/ml Heparin, 500 µg/ml tRNA, 0.1% Tween-20, 9.2 mM Citric acid, pH 6.0) without DIG-RNA probe at 68^{o}C for at least one hour. Hybridization was performed in hybridization solution containing DIG-labeled probe (1:200 dilution) at 68^{o}C for 16 hours.

Following to hybridization, the embryos were washed with 50% formamide /50% 2×SSC once for 5 minutes and then for 15 min at 68 ^{o}C, and then 2 x SSC once for 15 minutes at 68^{o}C, finally followed by the wash with 0.2xSSC twice for 30 minutes at 68^{o}C. After wash with PBST 5 x 5 min, the embryos were blocked with blocking solution of 2% normal sheep serum (NIPPON BIO-TEST LABORATORIES INC.), 2 mg/ml BSA at room temperature for one hour, and then incubated with anti-Digoxigenin-AP Fab fragments (Roche) (1:5000 dilution) in blocking solution for overnight at 4^{o}C. After the incubation, the embryos were washed with PBST five times for 15 minutes at room temperature, and then washed in coloration buffer (50 mM $MgCl_2$, 100 mM NaCl, 0.1% Tween20, 100 mM Tris-HCl, pH 9.5) at room temperature. DIG was detected with BM purple AP solution (Roche) at 4^{o}C

When the desired staining intensity was reached, the embryos were washed 3 x 5 minutes with PBST, then fixed in 4% PFA with 0.1% glutaraldehyde (Wako). After fixation, embryos were placed in 75 - 80% glycerol in PBS.

Two-color fluorescent in situ hybridization

DNP-labeled RNA probe was synthesized using T7 RNA polymerase (Roche) by incubating template DNA with 0.35 mM DNP-11-UTP (Perkin Elmer), 1 mM of ATP, GTP and CTP, 0.65 mM UTP (Invitrogen) for 3 hrs at 37^{o}C. The synthesized DNP-probe was purified by LiCl precipitation.

Embryos were prepared and hybridized with DIG-labeled and DNP-labeled riboprobe as described in WISH using AP-system, except for addition of 5% dextran sulfate (Sigma) to the hybridization buffer. The hybridized embryos were washed and blocked as WISH method of AP-system. After blocking, to detect DIG-labeled probe, the embryos were incubated with anti-digoxigenin-POD, Fab fragments (1:1000; Roche) in PBST containing 2% sheep serum and 2 mg/ml BSA for overnight at 4^{o}C. After the incubation, the embryos were washed 6 x 15 min in PBST and then 2 x 5 min in 1x amplification diluent, followed by the incubation with TSA

Plus Cyanine 5 solution (1:50 dilution in amplification diluent buffer) (Perkin Elmer) for 1 hr at R.T. After the incubation, embryos were washed 2 x 5 min with PBST and then the first TSA reaction was quenched in 2% H_2O_2 in PBST for 60 min at R.T. The embryos were then washed 4 x 5 min in PBST, followed by the incubation with anti-DNP-HRP (1:500; Perkin Elmer) in PBST containing 2% sheep serum and 2 mg/ml BSA for overnight at 4^{o}C. The antibody was washed out in PBST, and then the embryos were incubated in TSA Plus Cyanine 3 (1:50 dilution in amplification diluent buffer) (Perkin Elmer) for 1 hr at R.T. After the incubation, the embryos were washed 6 x 5 min in PBST and mounted in Prolong Diamond (Molecular probes) for imaging under confocal microscope.

Microscopy and image process

To observe and record the heart beating and the circulation, embryos/larvae were anesthetized using 0.012% MS-222 and were mounted either laterally or ventrally in 1.0% NuSive GTG Agarose (Lonza) on glass-bottomed 35 mm dish. Imaging was performed using a 10x dry objective lens (Plan Apo, NA0.45) or 20x multi immersion objective lens (Plan Fluor, NA0.75) (Nikon) mounted on Nikon A1R confocal microscope. Time-lapse image was recorded with a resonant scanner for 30 f/s imaging, and converted to QuickTime movie using IMARIS software (BITPLANE). These movies were converted into mp4 movies using iMovie software.

To take a image of whole mount in situ hybridization, specimens were mounted in 75 - 80% glycerol and imaged using 4 x (Plan Apo/NA0.20) or 10 x (Plan Apo/NA 0.45) (Nikon) objective lens mounted on Nikon eclipse inverted microscope and 1 x objective lens (Plan Apo) mounted on Leica M165 FC microscope.

To make a large image in Fig.1a, Fig. 3a, Figure S3, the tiled images of an embryo/larvae were taken using a 10x dry objective lens (Plan Apo, NA0.45) mounted on Nikon A1R confocal microscope. The obtained images were assembled using MosaicJ, a plugin of Image J. The assembled image was imported into Adobe Photoshop.

CRISPR/CAS9 mutagenesis

For CRISPR/Cas9, sgRNAs were designed using the online tool CHOPCHOP (http://chopchop.cbu.uib.no/#), CRISPR DESIGN (http://crispr.mit.edu/) and CRISPRdirect (https://crispr.dbcls.jp/). Target sequences and guide RNA (gRNA) sequences were listed in Table S2. For preparing gRNA, we followed either plasmid-based method, where the template sequence for gRNA was cloned in plasmid, or cloning-free method. For the plasmid based method (Jao et al., 2013), two complementary 20 μl base oligonucleotides corresponding to the target sequence were annealed in 20 μl solution with 1x NEBuffer3 by the following procedure: denaturation for 5 min at 95^{o}C, cooling to 50^{o}C at -0.1^{o}C /sec, pausing at 50 ^{o}C for 10 min and cooling to 4^{o}C at -0.1^{o}C /sec. One μl of annealed oligonucleotides was mixed with 400 ng of pT7-gRNA (Jao et al., 2013) (Addgene), which is a gRNA cloning vector, 0.5 μl of three restriction enzymes of BsmBI, BglII and SalI (NEB) each, 1 μl of 10x NEBuffer3 and 1 μl of T4 DNA ligase (NEB) in a volume of 20 μl to perform digestion and ligation in a single step. The oligonucleotides/enzymes mixture was incubated in three cycles of 20 min at 37^{o}C, 15 min at 16^{o}C, followed by 10 min at 37^{o}C and 15 min at 55^{o}C. Two μl of the reaction mixture was used to transform DH5α. After the preparation of plasmid using QIAprep Spin Miniprep Kit (QIAGEN) from several colonies, the successful cloning was confirmed by sequencing with M13Forward primer. The plasmid with gRNA target sequence was linearized by BamHI and used as a template of *in vitro* transcription reaction. gRNA was transcribed using MEGAshortscript kit (Ambion). The cloning-free method was also used to generate templates for gRNA synthesis (Gagnon et al., 2014). The 1 μl of 100 μM gene-specific oligonucleotides containing T7 or SP6 sequence, 20 base target sequence without PAM, and a complementary region to constant oligonucleotide were mixed with 1 μl of 100 μM oligonucleotide encoding the reverse-complement of the tracrRNA tail with 1x NEBuffer2 in a total volume of 10 μl to

anneal by the following procedure: denaturation for 5 min at 95°C, cooling to 85°C at -2°C /sec and then cooling from 85°C to 25°C at -0.1°C /sec. The single strand DNA overhangs were filled with T4 DNA polymerase by adding 2.5 μl 10 mM dNTPs mix, 1 μl 10x NEBuffer2, 0.2 μl 100x NEB BSA and 0.5 μl T4 DNA polymerase (NEB) and then incubated at 12°C for 20 min. The resulting double strand DNA was purified using QIAquick PCR purification kit (Qiagen). The gRNAs were transcribed using MEGAshortscript kit (Ambion). gRNAs were treated with DNase, which is included in the kit, and precipitated using lithium-chloride precipitation solution (Ambion). For making Cas9 mRNA to co-inject with gRNAs to zebrafish eggs, we used pCS2-nls-zCas9-nls(Jao et al., 2013) (Addgene) as a template DNA. The template DNA was linearized by NotI (NEB) and purified using QIAquick PCR purification kit. Capped nls-zCas9-nls mRNA was synthesized using mMESSAGE mMACHINE SP6 transcription kit (Ambion) in a volume of 20 μl. The synthesized mRNA was treated with DNase and precipitated with lithium-chloride precipitation solution (Ambion).

To assay and determine the indel mutation by gRNAs, the genome obtained from individual embryos of 1 to 4 dpf or tail clipping for direct sequencing and/or high resolution melt (HRM) analysis was used(Thomas et al., 2014). Embryo or tail fin clips were transferred into 25 to 50 μl of lysis buffer (10 mM Tris-HCl (pH 8.0), 50 mM KCl, 0.3% Tween20, 0.3% NP40, 1 mM EDTA, 0.2 mg/ml Proteinase K (Invitrogen)), and incubated at 55°C for 2 hrs to overnight, followed by the incubation at 98°C for 10 min. For direct sequence, the sequence spanning the gRNA target site was amplified by PCR using 1 μl of the lysed sample as a template, and purified the PCR product. Primers used for the PCR and direct sequencing are listed in Supplementary Table 2. For HRM analysis, we used LightCycler 480 High Resolution Melting Master (Roche) in combination with the LightCycler480 system (Roche). HRM reaction was performed in a volume of 10 μl containing 3.5 mM $MgCl_2$ and 0.2 μM each primer by running Gene Scanning 384-II program with the setting of annealing temperature of 60 to 63°C for the amplification and 5 sec hold time and 1°C /s ramp rate at 65°C for high resolution melting. The

results were analyzed using the programs of Gene Scanning, Melt Curve Genotyping and Tm calling in LightCycler480 software (Roche). Primers used for HRM analysis are listed in Table S2.

Rescue experiment

The pTol2(150/250):cmlc2(-210+34):MCS:polyA (pTol2:cmlc2:MCS:pA) plasmid (provided by Dr. Mochizuki) was used to construct pTol2:cmlc2: myl7-P2A-egfp, pTol2:cmlc2: cmlc1-P2A-egfp and pTol2:cmlc2: tnnc1a-P2A-egfp. The myl7, cmlc1 and tnnc1a sequences were amplified by PCR from 4 dpf zebrafish cDNA using following primers; For myl7, forward, 5'-CGCATCGAT(ClaI)GCCACCATGGCTAGTAAAAAAGCCGCGG-3', reverse, 5'-CGCGAATTC(EcoRI)AGATTCCTCTTTTTCATCACCATGTGTG-3', for cmlc1, forward, 5'- CGCATCGAT(ClaI)GCCACCATGGCACCAAAAAAAGTGGAACC-3', reverse, 5'-CGCGAATTC(EcoRI)CCCGGAGAGGATGTGCTTGATG-3', for tnnc1a, forward, 5'-CGCATCGAT(ClaI)GCCACCATGAACGACATCTACAAAGCAGC-3', reverse, 5'-CGCAAGCTT(HindIII)TTCCACCCCCTTCATGAACTCC-3'. P2A-egfp fragment amplified from pBluscript:P2A-egfp using primers; forward, 5'-CGCGAATTC(EcoRI)GGAAGCGGAGCTACTAACTTCAGC-3'(for fusion to myl7 and cmlc1) and 5'-CGCAAGCTT(HindIII)GGAAGCGGAGCTACTAACTTCAGC-3' (for fusion to tnnc1a) , reverse, 5'-CGCACTAGT(SpeI)TTACTTGTACAGCTCGTCCATGCC-3'. ClaI/SpeI-digested pTol2:cmlc2:MCS:pA vector was mixed with one of myl7, cmlc1 and tnnc1a fragments and P2A-egfp fragment to place myl7/cmlc1/tnnc1a-P2A-egfp sequence in the MCS of pTol2:cmlc2:MCS:pA. The pTol2:cmlc2:egfp was constructed by placing egfp sequence in the MCS of pTol2:cmlc2:MCS:pA. 10 ng/μl pTol2:cmlc2(myl7): myl7-P2A-egfp and pTol2:cmlc2:egfp were injected with 25 ng/μl transposase mRNA into one cell stage embryos obtained from myl7$^{+/+7bp}$, cmlc1$^{+/+29bp}$, tnnc1a$^{+/-5bp}$ allele mating.

Morpholino knockdown

Morpholinos were obtained from Gene Tools, LLC. A translation-blocking morpholino against etv2 (etsrp)(Pham et al., 2007) (5'-GGTTTTGACAGTGCCTCAGCTCTGC-3') targeting the -34 to -10 region of the etv2 (etsrp) sequences was used. The morpholino solution with the concentration of 2 ng/µl was injected to one-cell embryos obtained from *Tg(fli1a:egfp)* and *Tg(gata1:DsRed)* mating. Embryos were harvested on 2 dpf for the analyses.

Atorvastatin treatment

Atorvastatin Calcium Trihydrate (Wako) was dissolved in 100% DMSO at a concentration of 10 mM. Drug was diluted in 0.001% PTU to make the working solution of 2 µM with 0.2% DMSO. Atorvastatin treatment was initiated at 24 hpf and replaced with fresh drug every 24 hrs to 4.5 dpf. To combine atorvastatin treatment and heart ablation, embryos were first treated with atorvastatin to 3 dpf. Then the embryos were soaked in the mixture of 2 µM atorvastatin and 10 mM MTZ for 6 hrs at 3 dpf, followed by the incubation in atorvastatin solution again to 4.5 dpf.

Data analyses and statistics

For data collection and analysis of qRT-PCR, no statistical methods were used to predetermine sample size. Embryos/larvae subjected to qRT-PCR analysis were blindly collected from cluchmates. The etv2 morphants were identified by the reduced expression of *Tg(fli1a:egfp)* reporter and processed for the analyses. For collecting larvae in Figure S4, those expressing GFP widely in heart (more than 70% in heart in appearance under fluorescence stereo microscope) were collected for qRT-PCR analysis. For qRT-PCR data analysis of mutant fish of myl7, cmlc1, tnnc1a and dpys in Fig. 1 and Fig. 2, values of 2^{-dCt} obtained from two different mutant alleles of each gene were combined to calculate statistics. Because the expression level of lepb gene in wild type embryo/larva was extremely low, a signal of SYBR Green was not detected in our experimental design of qRT-PCR in most of WT. Therefore, in Figs 1, 2 and 4,

and Figure S9, we considered the Ct of lepb as 46, if the signal was not detected. Ora1 gene also showed a similarly low expression in WT – the signals for one of eight WTs and one of eight cloche mutants with MTZ treatment were undetectable. Thus, for these samples, the Ct was also considered as 46. For drug treatment in Figure S10, embryos/larvae were randomly selected and processed for each treatment group. For the WISH experiments, at least 8 individual fish were processed and examined. Student t-test was performed for statistical analysis, and a p-value less than 0.05 was considered to be statistically significant (* $p<0.05$, ** $p<0.01$ and *** $p<0.001$). The horizontal line represents the mean.

SUPPLEMENTARY INFORMATION

Supplementary Information includes 10 figures, 2 tables and 8 movies and can be found with this article online.

AUTHOR CONTRIBUTIONS

T.N.S. conceived the idea of the project, designed the overall experiments and *in silico* analyses and supervised the overall research project. N.T. and M.O. contributed to designing the experiments and performed the experiments. S.K. performed the in silico analyses. F.S. and S.E. contributed to the experiments. N.C.C. developed *Tg(cmlc2:mcherry-NTR)* zebrafish line. T.N.S., N.T., M.O., S.K. wrote the manuscript.

ACKNOWLEDGEMENTS

We thank Y. Oka, T. Ninomiya, T. Kuroda, H. Anabuki for technical assistance, R. Takahashi, E. Kojima for administrative assistance, T. Morie for managing the laboratory's daily operations. J.H. Neale and S. Kawaoka read the manuscript draft versions and provided critical and constructive comments on the manuscript. We are also grateful to the Sato lab members for advice and discussion throughout the course of this work. M.O. has completed this work as part of her Ph.D. dissertation requirement. This work was supported by JST ERATO (T.N.S.), JSPS KAKENHI S Grant Number 22229007 (T.N.S.).

COMPETING INTERESTS

The authors declare no competing financial interests.

REFERENCES

Aaronson, P.I., Ward, J.P.T., and Connolly, M.J. (2014). The cardiovascular system at a glance, 4th edition edn (United States: Wiley-Blackwell).

Afgan, E., Baker, D., van den Beek, M., Blankenberg, D., Bouvier, D., Cech, M., Chilton, J., Clements, D., Coraor, N., Eberhard, C.*, et al.* (2016). The Galaxy platform for accessible, reproducible and collaborative biomedical analyses: 2016 update. Nucleic acids research *44*, W3-W10.

Ahuja, G., and Korsching, S. (2014). Zebrafish olfactory receptor ORA1 recognizes a putative reproductive pheromone. Communicative & integrative biology *7*.

Anderson, J.L., Carten, J.D., and Farber, S.A. (2011). Zebrafish lipid metabolism: from mediating early patterning to the metabolism of dietary fat and cholesterol. Methods in cell biology *101*, 111-141.

Behrens, M., Frank, O., Rawel, H., Ahuja, G., Potting, C., Hofmann, T., Meyerhof, W., and Korsching, S. (2014). ORA1, a zebrafish olfactory receptor ancestral to all mammalian V1R genes, recognizes 4-hydroxyphenylacetic acid, a putative reproductive pheromone. The Journal of biological chemistry *289*, 19778-19788.

Celik, A., Fuss, S.H., and Korsching, S.I. (2002). Selective targeting of zebrafish olfactory receptor neurons by the endogenous OMP promoter. The European journal of neuroscience *15*, 798-806.

Craig, M.P., Grajevskaja, V., Liao, H.K., Balciuniene, J., Ekker, S.C., Park, J.S., Essner, J.J., Balciunas, D., and Sumanas, S. (2015). Etv2 and fli1b function together as key regulators of vasculogenesis and angiogenesis. Arteriosclerosis, thrombosis, and vascular biology *35*, 865-876.

Curado, S., Anderson, R.M., Jungblut, B., Mumm, J., Schroeter, E., and Stainier, D.Y. (2007). Conditional targeted cell ablation in zebrafish: a new tool for regeneration studies. Developmental dynamics : an official publication of the American Association of Anatomists

236, 1025-1035.

Curado, S., Stainier, D.Y., and Anderson, R.M. (2008). Nitroreductase-mediated cell/tissue ablation in zebrafish: a spatially and temporally controlled ablation method with applications in developmental and regeneration studies. Nature protocols *3*, 948-954.

D'Amico, L., Scott, I.C., Jungblut, B., and Stainier, D.Y. (2007). A mutation in zebrafish hmgcr1b reveals a role for isoprenoids in vertebrate heart-tube formation. Current biology : CB *17*, 252-259.

Dhakal, S., Stevens, C.B., Sebbagh, M., Weiss, O., Frey, R.A., Adamson, S., Shelden, E.A., Inbal, A., and Stenkamp, D.L. (2015). Abnormal retinal development in Cloche mutant zebrafish. Developmental dynamics : an official publication of the American Association of Anatomists *244*, 1439-1455.

Dickover, M.S., Zhang, R., Han, P., and Chi, N.C. (2013). Zebrafish cardiac injury and regeneration models: a noninvasive and invasive in vivo model of cardiac regeneration. Methods in molecular biology *1037*, 463-473.

Droujinine, I.A., and Perrimon, N. (2013). Defining the interorgan communication network: systemic coordination of organismal cellular processes under homeostasis and localized stress. Frontiers in cellular and infection microbiology *3*, 82.

Fernandes, A.M., Beddows, E., Filippi, A., and Driever, W. (2013). Orthopedia transcription factor otpa and otpb paralogous genes function during dopaminergic and neuroendocrine cell specification in larval zebrafish. PloS one *8*, e75002.

Gagnon, J.A., Valen, E., Thyme, S.B., Huang, P., Akhmetova, L., Pauli, A., Montague, T.G., Zimmerman, S., Richter, C., and Schier, A.F. (2014). Efficient mutagenesis by Cas9 protein-mediated oligonucleotide insertion and large-scale assessment of single-guide RNAs. PloS one *9*, e98186.

Ho, S.Y., Thorpe, J.L., Deng, Y., Santana, E., DeRose, R.A., and Farber, S.A. (2004). Lipid metabolism in zebrafish. Methods in cell biology *76*, 87-108.

Isogai, S., Lawson, N.D., Torrealday, S., Horiguchi, M., and Weinstein, B.M. (2003). Angiogenic network formation in the developing vertebrate trunk. Development *130*, 5281-5290.

Jao, L.E., Wente, S.R., and Chen, W. (2013). Efficient multiplex biallelic zebrafish genome editing using a CRISPR nuclease system. Proceedings of the National Academy of Sciences of the United States of America *110*, 13904-13909.

Kimmel, C.B., Ballard, W.W., Kimmel, S.R., Ullmann, B., and Schilling, T.F. (1995). Stages of embryonic development of the zebrafish. Developmental dynamics : an official publication of the American Association of Anatomists *203*, 253-310.

Korzh, S., Pan, X., Garcia-Lecea, M., Winata, C.L., Pan, X., Wohland, T., Korzh, V., and Gong, Z. (2008). Requirement of vasculogenesis and blood circulation in late stages of liver growth in zebrafish. BMC developmental biology *8*, 84.

Lammert, E., Cleaver, O., and Melton, D. (2001). Induction of pancreatic differentiation by signals from blood vessels. Science *294*, 564-567.

Langmead, B., and Salzberg, S.L. (2012). Fast gapped-read alignment with Bowtie 2. Nature methods *9*, 357-359.

Lawson, N.D., and Weinstein, B.M. (2002). In vivo imaging of embryonic vascular development using transgenic zebrafish. Developmental biology *248*, 307-318.

Liao, W., Bisgrove, B.W., Sawyer, H., Hug, B., Bell, B., Peters, K., Grunwald, D.J., and Stainier, D.Y. (1997). The zebrafish gene cloche acts upstream of a flk-1 homologue to regulate endothelial cell differentiation. Development *124*, 381-389.

Love, M.I., Huber, W., and Anders, S. (2014). Moderated estimation of fold change and dispersion for RNA-seq data with DESeq2. Genome biology *15*, 550.

Lu, L., Chen, Y., Wang, Z., Li, X., Chen, W., Tao, Z., Shen, J., Tian, Y., Wang, D., Li, G.*, et al.* (2015). The goose genome sequence leads to insights into the evolution of waterfowl and susceptibility to fatty liver. Genome biology *16*, 89.

Mathews, E.S., Mawdsley, D.J., Walker, M., Hines, J.H., Pozzoli, M., and Appel, B. (2014). Mutation of 3-hydroxy-3-methylglutaryl CoA synthase I reveals requirements for isoprenoid and cholesterol synthesis in oligodendrocyte migration arrest, axon wrapping, and myelin gene expression. The Journal of neuroscience : the official journal of the Society for Neuroscience *34*, 3402-3412.

Matsumoto, K., Yoshitomi, H., Rossant, J., and Zaret, K.S. (2001). Liver organogenesis promoted by endothelial cells prior to vascular function. Science *294*, 559-563.

Mazein, A., Watterson, S., Hsieh, W.Y., Griffiths, W.J., and Ghazal, P. (2013). A comprehensive machine-readable view of the mammalian cholesterol biosynthesis pathway. Biochemical pharmacology *86*, 56-66.

Myers, M.G., Jr., and Olson, D.P. (2012). Central nervous system control of metabolism. Nature *491*, 357-363.

Nellore, A., Jaffe, A.E., Fortin, J.P., Alquicira-Hernandez, J., Collado-Torres, L., Wang, S., Phillips Iii, R.A., Karbhari, N., Hansen, K.D., Langmead, B.*, et al.* (2016). Human splicing diversity and the extent of unannotated splice junctions across human RNA-seq samples on the Sequence Read Archive. Genome biology *17*, 266.

Noble, M. (2002). The cardiovascular system in health and disease (London, UK: Imperial College Press).

Paton, C.M., and Ntambi, J.M. (2009). Biochemical and physiological function of stearoyl-CoA desaturase. American journal of physiology Endocrinology and metabolism *297*, E28-37.

Pham, V.N., Lawson, N.D., Mugford, J.W., Dye, L., Castranova, D., Lo, B., and Weinstein, B.M. (2007). Combinatorial function of ETS transcription factors in the developing vasculature. Developmental biology *303*, 772-783.

Rajan, A., and Perrimon, N. (2011). Drosophila as a model for interorgan communication: lessons from studies on energy homeostasis. Developmental cell *21*, 29-31.

Reischauer, S., Stone, O.A., Villasenor, A., Chi, N., Jin, S.W., Martin, M., Lee, M.T., Fukuda,

N., Marass, M., Witty, A., *et al.* (2016). Cloche is a bHLH-PAS transcription factor that drives haemato-vascular specification. Nature *535*, 294-298.

Stainier, D.Y. (2001). Zebrafish genetics and vertebrate heart formation. Nature reviews Genetics *2*, 39-48.

Sumanas, S., and Lin, S. (2006). Ets1-related protein is a key regulator of vasculogenesis in zebrafish. PLoS Biol *4*, e10.

Thomas, H.R., Percival, S.M., Yoder, B.K., and Parant, J.M. (2014). High-throughput genome editing and phenotyping facilitated by high resolution melting curve analysis. PloS one *9*, e114632.

Trapnell, C., Williams, B.A., Pertea, G., Mortazavi, A., Kwan, G., van Baren, M.J., Salzberg, S.L., Wold, B.J., and Pachter, L. (2010). Transcript assembly and quantification by RNA-Seq reveals unannotated transcripts and isoform switching during cell differentiation. Nature biotechnology *28*, 511-515.

Traver, D., Paw, B.H., Poss, K.D., Penberthy, W.T., Lin, S., and Zon, L.I. (2003). Transplantation and in vivo imaging of multilineage engraftment in zebrafish bloodless mutants. Nature immunology *4*, 1238-1246.

Veldman, M.B., and Lin, S. (2012). Etsrp/Etv2 is directly regulated by Foxc1a/b in the zebrafish angioblast. Circulation research *110*, 220-229.

Weinstein, B.M. (2002). Plumbing the mysteries of vascular development using the zebrafish. Seminars in cell & developmental biology *13*, 515-522.

Weinstein, B.M. (2005). Vessels and nerves: marching to the same tune. Cell *120*, 299-302.

Weinstein, B.M., and Fishman, M.C. (1996). Cardiovascular morphogenesis in zebrafish. Cardiovascular research *31 Spec No*, E17-24.

FIGURE LEGENDS

Figure 1. The bodywide transcriptome landscape of "heartless" and cardiac gene mutants.

a. Generation of "heartless". Scale bars: 400 μm (top panel), 200 μm (middle panels), 50 μm (bottom panels). Red: cardiomyocyte. Green: vascular endothelial-cells (ECs) and endocardium. **b.** GO enrichment analysis of "heartless". The top 20 GO terms are shown. **c.** Volcano plot of the gene expression in "heartless". Red: Upregulated. Blue: Downregulated. n=2. **d.** Cardiac-gene (myl7, cmlc1, tnnc1a) mutants. The expression patterns shown as a heatmap. ■ $p \geqq 0.05$. Student t-test. n=16 – 21. **e.** The bodywide transcriptome landscape of "heartless". The cardiac-mechanism (I- VI) (right panel) is indicated for each gene (left panel). Others: other organs/tissues. N.D.: expression sites not determined. A, atrium; V, ventricle; Oft, outflow tract.

Figure 2. The bodywide transcriptome landscape of liver-gene mutants. a. The heatmap of gene expression patterns for each mutant. For c3b and cfb mutants, the results for both DMSO- (mutant) and MTZ- (mutant and "heartless" double) treated larvae are shown. ■$p \geqq 0.05$. n=8 – 13. **b.** The bscl2l expression in wild type (WT) and dpys mutant (-/-). ***$p<0.001$, n.s.: not significant. n=8 (WT, 4.5 dpf), 11 ($dpys^{-/-}$, 4.5 dpf), 5 (WT, 10 dpf), 10 ($dpys^{-/-}$, 10 dpf), 25 (WT, 30 dpf), 17 ($dpys^{-/-}$, 30 dpf). **c.** The bscl2l expression in each organ of wild type (WT) and dpys mutant (-/-). The expression level in the heart, the kidney, the liver, the intestine, the pancreas, and the remaining body parts are normalized by myl7, cdh17, fabp10a, fabp2, ctrb1, and rpl13a, respectively. *$p<0.05$, n.s.: not significant. n=4 (heart, liver, intestine, pancreas, WT remaining body), n=3 (kidney, $dpys^{-/-}$remaining body). **d.** The hierarchical map. Dotted blue lines/arrows indicate weak interactions. The solid blue line indicates the strong interaction. Heat gradient, ■ (cbln14 in $rbp2b^{-/-}$) indicates no PCR amplifications with 6 out of 8 samples.

Figure 3. The bodywide transcriptome landscape of "vesselless". a. Use of *cloche* mutant (*cloche*$^{-/-}$) as "vesselless". Red: cardiomyocyte. Green: vascular endothelial-cells (ECs) and

endocardium of the heart. Scale bar, 100 μm. **b.** GO enrichment analysis of "vesselless" (blue) and "heartless" (red). The top 44 GO terms are shown. **c.** Volcano plot. Red: Differentially expressed genes in "heartless". Blue: The genes that are affected in "vesselless", but not in "heartless". n=2. **d.** WISH patterns of genes encoding cholesterol biosynthesis. Arrows: Liver. Arrowheads: Intestine. *: Brain. Scale bar, 500 μm. **e.** WISH patterns of olfactory-specific genes, ompa, ompb and ora1. Scale bar, 100 μm. Double WISH staining for ompa and ompb (bottom). Green: ompa. Red: ompb. Scale bar, 15 μm. Dotted white line, olfactory bulb. **f.** Correlational plot of "vesselless" and etv2 morphant (etv2 MO). R^2=0.81821. n=17 (WT), n=22 (MO), n=8 ("vesselless"), n=8 (sibling control). **g.** The bodywide transcriptome landscape of "vesselless".

Figure 4. Mechanistic models. a. Models. **b.** Flowchart of the algorithm (left panel) and the simulation results (right panel). Red: Upregulation. Blue: Downregulation. **c.** Experimental results shown as heatmap. ■p≧0.05. n=8. **d.** Summary. Each gene is assigned to each mechanistic category (M1, M2, M3, M4) based on the experimental results. Those that could not be assigned onto any categories are indicated by yellow. The thresholds for the up or down in the expression levels are set at x1.5 or x0.66, respectively. *indicates those of which expression levels change less than x1.5 -fold or more than x0.66, but exhibit statistically significant (i.e., $p<0.05$) changes.

Figure 5. The bodywide landscape depicting the relationship of each gene and the mechanistic underpinnings. Each gene is placed according to the site(s) of its expression and the mechanism(s) (A – H & I – VI) for its differential expression. Gene-to-gene coregulations are indicated by dotted arrows. *indicates those of which expression levels change only x0.5 – x2, but exhibit statistically significant (i.e., $p<0.05$) change.

SUPPLEMENTARY INFORMATION

Figure S1. WISH expression patterns of the genes. The patterns are shown for wild type (WT) and "heartless" larvae at 4.5 dpf for each gene. **a.** Liver genes. **b.** Liver/kidney genes. The renal expression of dpys in 4.5 dpf larva is shown by co-staining with a marker for proximal convoluted tubule, slc20a1a. **c.** Genes expressed in the liver, somite and others. **d.** Somite gene. qRT-PCR result (top graph) shows the higher expression of tgm2a at 3.5 dpf. **e.** Pancreas gene. **d.** Genes expressed in tissues/organs that are undefined (Others). Scale bars, 500 μm.

Figure S2. WISH expression patterns of the other genes. a. Liver genes. **b.** Genes expressed in both the liver and kidney. **c.** Genes expressed in the liver and tissues/organs that are undefined (Others). **d.** Genes whose expressions are not determined (N.D.). Scale bars, 500 μm.

Figure S3. Liver genes. a. Generation of "liverless". Scale bars, 500 μm. Arrowheads denote fluorescent (Cyan) liver. **b.** Volcano plot of the bodywide transcriptome data of "liverless" showing the liver genes (red). Their expression was significantly reduced in "liverless", except two genes (igfbp1a and hamp). However, their expression in the liver was confirmed by WISH (Extended Data Fig. 1a). It is possible that they are upregulated in the small residual liver tissues in "liverless".

Figure S4. Cardiac gene mutants and their genetic rescue. a. CRSIPR/Cas9 mediated mutation strategies for myl7, cmlc1 and tnnc1a. **b.** Mutations introduced in myl7, cmlc1 and tnnc1a genome. **c.** Genetic rescue strategy. **d.** Correlational plots for WT/Mutant and Rescued/Mutant. Complete (R^2=0.95501), partial (R^2=0.76025) and no rescues (R^2=0.00994) by myl7 promoter-driven re-introduction of myl7 (n=8), cmlc1 (n=3 for the rescue experiment, n=4 for the control cmlc1$^{-/-}$), WT and tnnc1a (n=8), respectively.

Figure S5. Generation and characterization of the liver-gene-mutants. a. CRSIPR/Cas9 mediated mutation strategies for cbln13, cbln8, dpys, fabp10a, rbp2b, ahsg1, ugt1a5, c3b, cfb, tgm2a and uox. **b.** Mutations introduced into their genomes. **c.** Purities of each isolated organ. The purities of the heart, the kidney, the liver, the intestine, the pancreas are evaluated by measuring the expressions of myl7, cdh17, fabp10a, fabp2 and ctrb1, respectively, by qRT-PCR. For the evaluation of the remaining body, a neuronal marker, elavl3, are used. n=3 - 4. **d.** The qRT-PCR analysis of bscl2l expression in each purified organ is shown. n=3 - 4.

Figure S6. The pathways for cholesterol biosynthesis. The genes specifically reduced in "vesselless" (i.e., cloche$^{-/-}$) are in red.

Figure S7. Reduced vasculature in etv2 morphant. The vasculature of *cloche*$^{+/?}$, *cloche*$^{-/-}$ (i.e., "vesselless") and etv2 morphant is compared by fli1a:egfp signals. Scale bars, 500 μm.

Figure S8. Pseudocode for the flowchart in Fig. 4a.

Figure S9. Generation and characterization of double mutant for otpa and otpb genes. a. CRSIPR/Cas9 mediated mutation strategies for otpa and otpb genes. **b.** Mutations introduced into otpa and otpb genome. **c.** The expressions of the genes in categories E and F in the otpa/otpb double mutant. *p<0.05, **p<0.01, ***p<0.001, n.s., not significant. Student-t test. n=6(WT), n=7(otpa$^{-/-}$;otpb$^{-/-}$).

Figure S10. The expression of the genes encoding enzymes for cholesterol biosynthesis in statin-treated larvae. The qRT-PCR results showing the expressions of each gene in control (WT), atorvastatin-treated control (WT+Statin), "heartless" (Heartless), atorvastatin-treated "heartless" (Heartless+Statin), "vesselless" (Vesselless) and atorvastatin-treated "vesselless"

(Vesselless+Statin) larvae . *p<0.05, **<0.01, ***p<0.001, n.s., not significant, n=8.

Table S1. This excel table contains qRT-PCR data (Fig. 1c, Dissected liver, Fig. 1d, Figure S4d, Figs. 2a, 2b, 2c, Figures. S5c, d, Figs. 3f, 4c, Figures S9c, S10) used in this study and full GO terms (Fig. 1b & Fig. 3b).

Table S2. This excel table contains a list of genes, primers, riboprobes, and gRNAs used in this study.

Movie S1. This video shows cardiac contraction and circulation of wild type.

Movie S2. This video shows the lack of cardiac contraction and circulation of myl7 mutant.

Movie S3. This video shows the lack of cardiac contraction and circulation of cmlc1 mutant.

Movie S4. This video shows aberrant cardiac contraction and circulation of tnnc1a mutant.

Movie S5. This video shows normal rescued cardiac contraction and circulation of the myl7 mutant.

Movie S6. This video shows partially rescued cardiac contraction but no circulation of the cmlc1 mutant.

Movie S7. This video shows the lack of cardiac contraction and circulation of the tnnc1a mutant following the re-introduction of tnnc1a via the myl7 promoter.

Movie S8. This video shows cardiac contraction without endocardium but no circulation of "vesselless" (cloche$^{-/-}$).

Figure 1

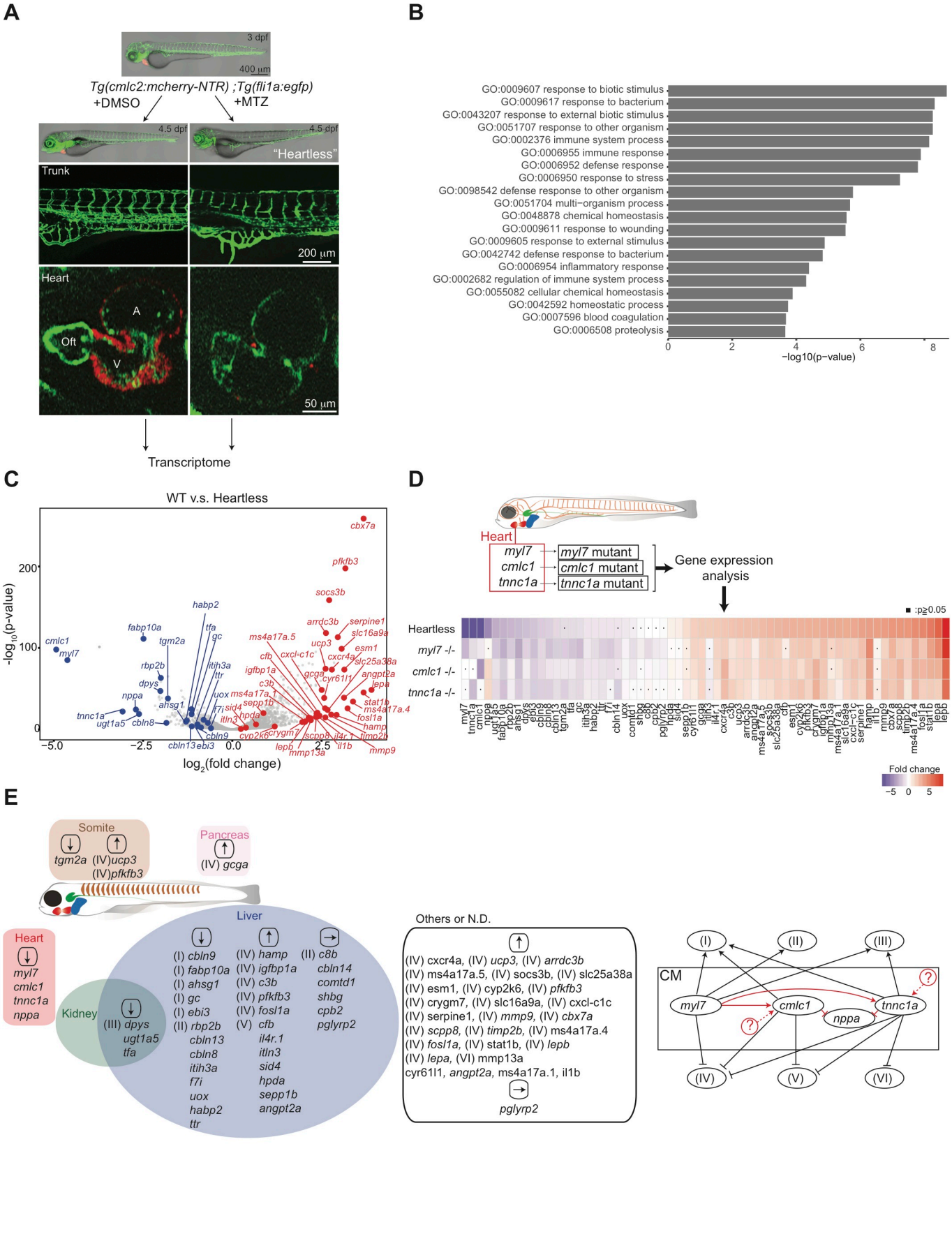
A
3 dpf
400 μm
Tg(cmlc2:mcherry-NTR) ;Tg(fli1a:egfp)
+DMSO
+MTZ
4.5 dpf
4.5 dpf
"Heartless"
Trunk
200 μm
Heart
A
Oft
V
50 μm
Transcriptome
B
GO:0009607 response to biotic stimulus
GO:0009617 response to bacterium
GO:0043207 response to external biotic stimulus
GO:0051707 response to other organism
GO:0002376 immune system process
GO:0006955 immune response
GO:0006952 defense response
GO:0006950 response to stress
GO:0098542 defense response to other organism
GO:0051704 multi−organism process
GO:0048878 chemical homeostasis
GO:0009611 response to wounding
GO:0009605 response to external stimulus
GO:0042742 defense response to bacterium
GO:0006954 inflammatory response
GO:0002682 regulation of immune system process
GO:0055082 cellular chemical homeostasis
GO:0042592 homeostatic process
GO:0007596 blood coagulation
GO:0006508 proteolysis
0
2
4
6
8
−log10(p−value)
C
WT v.s. Heartless
-log10(p-value)
log2(fold change)
D
Heart
myl7
cmlc1
tnnc1a
myl7 mutant
cmlc1 mutant
tnnc1a mutant
Gene expression analysis
■ :p≧0.05
Heartless
myl7 -/-
cmlc1 -/-
tnnc1a -/-
Fold change
E
Somite
tgm2a
(IV)ucp3
(IV)pfkfb3
Pancreas
(IV) gcga
Liver
Heart
myl7
cmlc1
tnnc1a
nppa
Kidney
(III) dpys
ugt1a5
tfa
(I) cbln9
(I) fabp10a
(I) ahsg1
(I) gc
(I) ebi3
(II) rbp2b
cbln13
cbln8
itih3a
f7i
uox
habp2
ttr
(IV) hamp
(IV) igfbp1a
(IV) c3b
(IV) pfkfb3
(IV) fosl1a
(V) cfb
il4r.1
itln3
sid4
hpda
sepp1b
angpt2a
(II) c8b
cbln14
comtd1
shbg
cpb2
pglyrp2
Others or N.D.
(IV) cxcr4a, (IV) ucp3, (IV) arrdc3b
(IV) ms4a17a.5, (IV) socs3b, (IV) slc25a38a
(IV) esm1, (IV) cyp2k6, (IV) pfkfb3
(IV) crygm7, (IV) slc16a9a, (IV) cxcl-c1c
(IV) serpine1, (IV) mmp9, (IV) cbx7a
(IV) scpp8, (IV) timp2b, (IV) ms4a17a.4
(IV) fosl1a, (IV) stat1b, (IV) lepb
(IV) lepa, (VI) mmp13a
cyr61l1, angpt2a, ms4a17a.1, il1b
pglyrp2
CM
myl7
cmlc1
nppa
tnnc1a
(I)
(II)
(III)
(IV)
(V)
(VI)

Figure 2

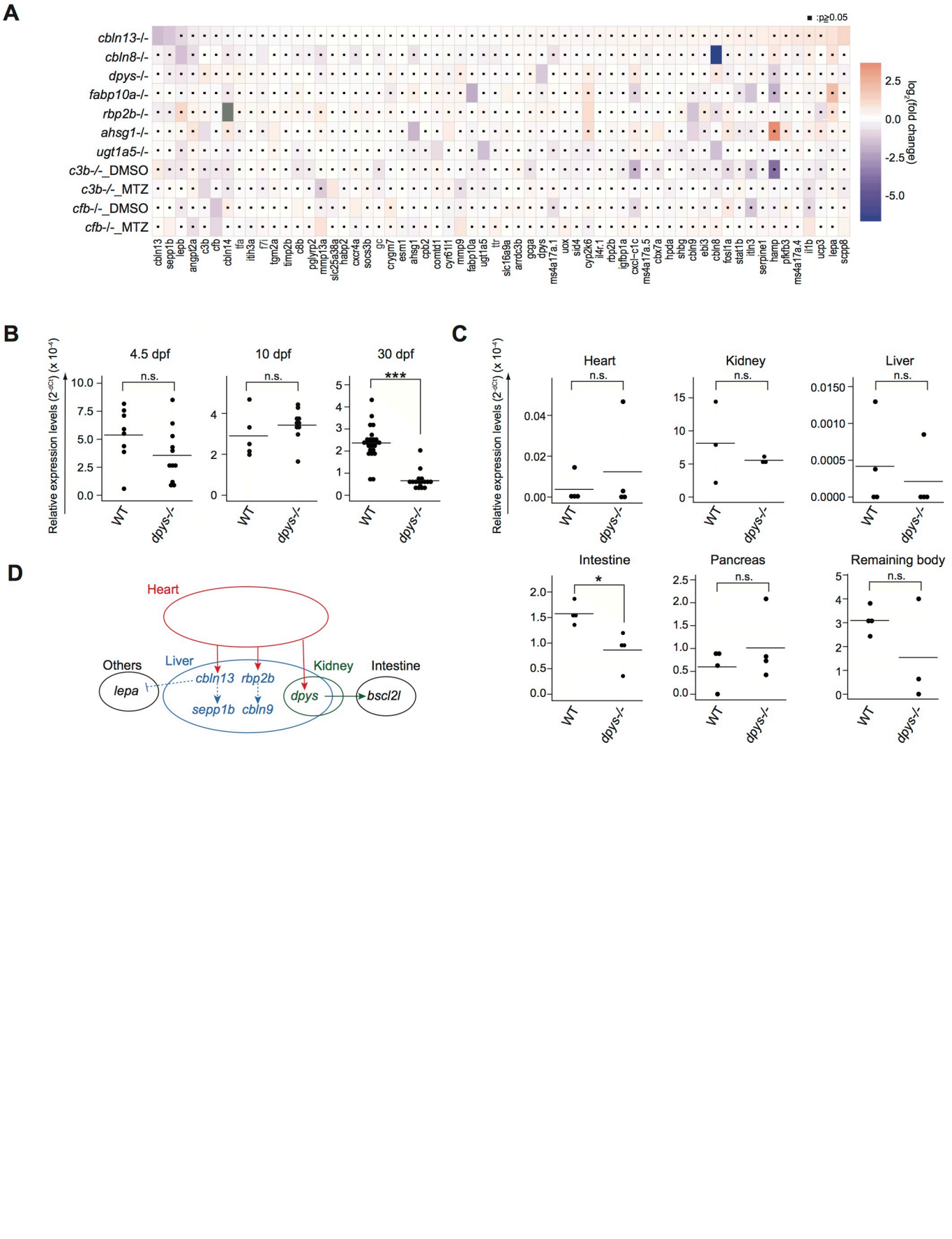
A
■ :p≧0.05
cbln13-/-
cbln8-/-
dpys-/-
fabp10a-/-
rbp2b-/-
ahsg1-/-
ugt1a5-/-
c3b-/-_DMSO
c3b-/-_MTZ
cfb-/-_DMSO
cfb-/-_MTZ
log2(fold change)
2.5
0.0
-2.5
-5.0
cbln13 sepp1b lepb angpl2a c3b cfb cbln14 tfa itih3a f7i tgm2a timp2b c8b pglyrp2 mmp13a slc25a38a habp2 cxcr4a socs3b gc crygm7 esm1 ahsg1 cpb2 comtd1 cyr61l1 mmp9 fabp10a ugt1a5 ttr slc16a9a arrdc3b gcga dpys ms4a17a.1 uox sid4 cyp2k6 il4r.1 rbp2b igfbp1a cxcl-c1c ms4a17a.5 cbx7a hpda shbg cbln9 ebi3 cbln8 fosl1a stat1b itln3 serpine1 hamp pkfb3 ms4a17a.4 il1b ucp3 lepa scpp8
B
Relative expression levels (2-dCt) (x 10-4)
4.5 dpf
10 dpf
30 dpf
n.s.
n.s.
***
WT
dpys-/-
C
Heart
Kidney
Liver
Intestine
Pancreas
Remaining body
n.s.
*
D
Heart
Others
Liver
Kidney
Intestine
lepa
cbln13
rbp2b
sepp1b
cbln9
dpys
bscl2l

Figure 3

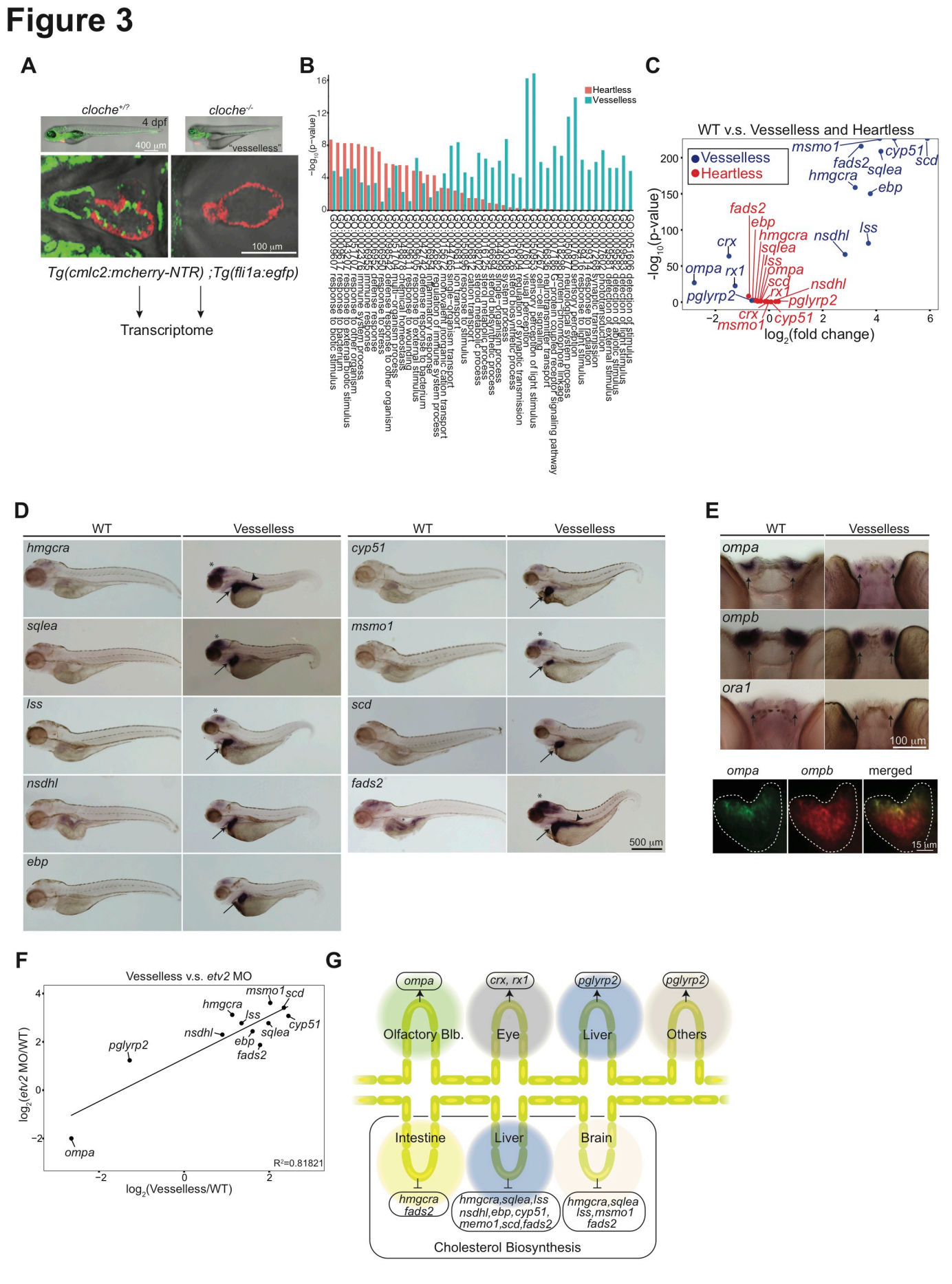
A
cloche+/?
cloche-/-
4 dpf
400 μm
"vesselless"
100 μm
Tg(cmlc2:mcherry-NTR) ;Tg(fli1a:egfp)
Transcriptome
B
Heartless
Vesselless
−log10(p-value)
C
WT v.s. Vesselless and Heartless
Vesselless
Heartless
-log10(p-value)
log2(fold change)
msmo1
cyp51
fads2
sqlea
scd
hmgcra
ebp
lss
nsdhl
crx
rx1
ompa
pglyrp2
D
WT
Vesselless
hmgcra
cyp51
sqlea
msmo1
lss
scd
nsdhl
fads2
ebp
500 μm
E
WT
Vesselless
ompa
ompb
ora1
100 μm
ompa
ompb
merged
15 μm
F
Vesselless v.s. etv2 MO
log2(etv2 MO/WT)
log2(Vesselless/WT)
R²=0.81821
msmo1
scd
hmgcra
lss
cyp51
nsdhl
ebp
sqlea
fads2
pglyrp2
ompa
G
ompa
crx, rx1
pglyrp2
pglyrp2
Olfactory Blb.
Eye
Liver
Others
Intestine
Liver
Brain
hmgcra
fads2
hmgcra,sqlea,lss
nsdhl,ebp,cyp51,
memo1,scd,fads2
hmgcra,sqlea
lss,msmo1
fads2
Cholesterol Biosynthesis

Figure 4

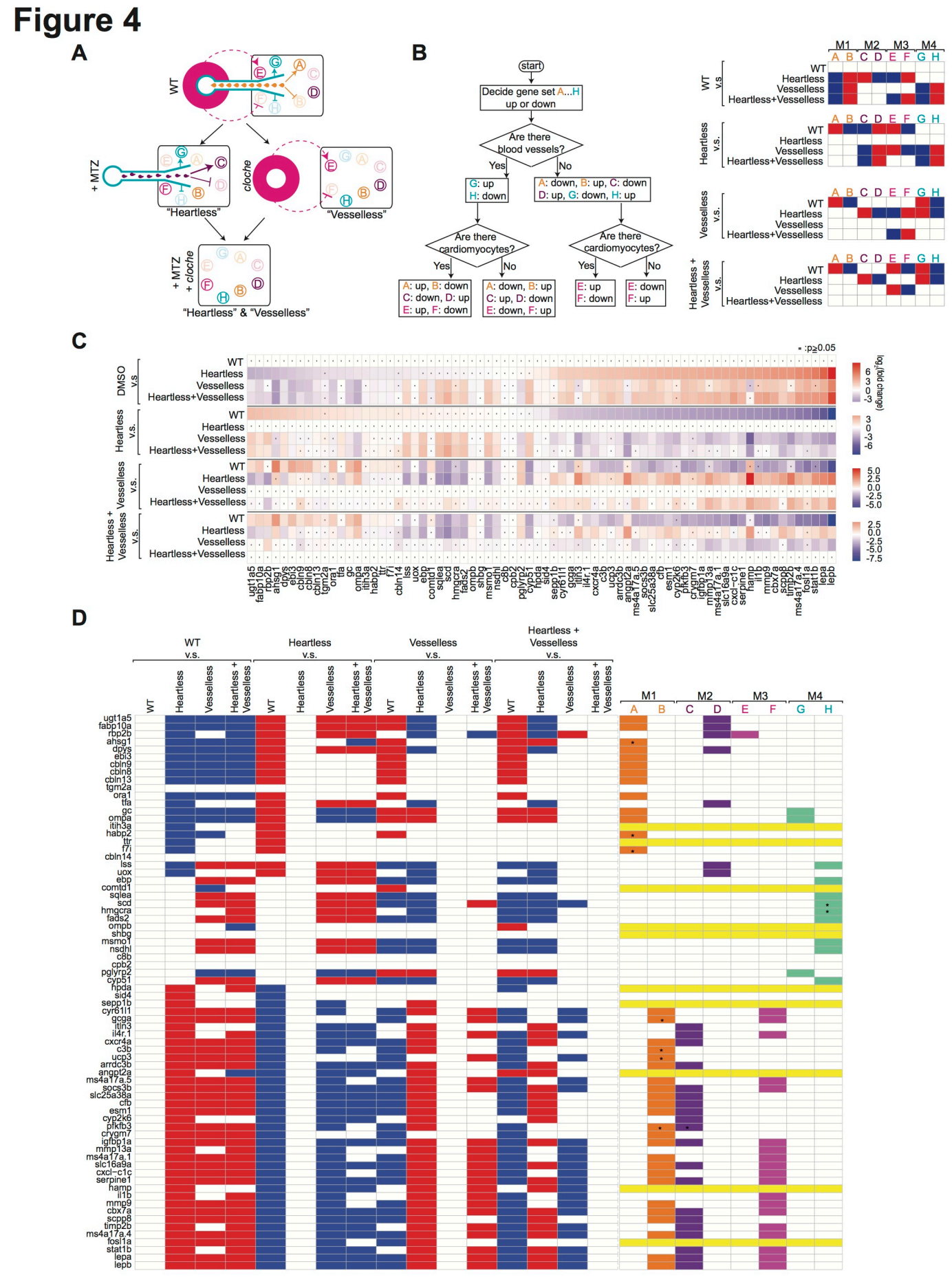
A
WT
+ MTZ
cloche
"Heartless"
"Vesselless"
+ MTZ
+ cloche
"Heartless" & "Vesselless"
B
start
Decide gene set A...H up or down
Are there blood vessels?
Yes
No
G: up
H: down
A: down, B: up, C: down
D: up, G: down, H: up
Are there cardiomyocytes?
A: up, B: down
C: down, D: up
E: up, F: down
A: down, B: up
C: up, D: down
E: down, F: up
E: up
F: down
E: down
F: up
M1 M2 M3 M4
A B C D E F G H
WT v.s.
Heartless v.s.
Vesselless v.s.
Heartless + Vesselless v.s.
WT
Heartless
Vesselless
Heartless+Vesselless
C
▪ :p≥0.05
log2(fold change)
DMSO v.s.
Heartless v.s.
Vesselless v.s.
Heartless + Vesselless v.s.
WT
Heartless
Vesselless
Heartless+Vesselless
ugt1a5 fabp10a rbp2b ahsg1 dpys ebi3 cbln9 cbln8 cbln13 tgm2a ora1 tfa gc ompa itih3a habp2 ttr f7i cbln14 lss uox ebp comtd1 sqlea scd hmgcra fads2 ompb shbg msmo1 nsdhl c8b cpb2 pglyrp2 cyp51 hpda sid4 sepp1b cyr61l1 gcga itih3 il4r1 cxcr4a c3b ucp3 arrdc3b angpt2a ms4a17a.5 socs3b slc25a38a cfb esm1 cyp2k6 pfkfb3 crygm7 igfbp1a mmp13a ms4a17a.1 slc16a9a cxcl−c1c serpine1 hamp il1b mmp9 cbx7a scpp8 timp2b ms4a17a.4 fosl1a stat1b lepa lepb
D
WT v.s.
Heartless v.s.
Vesselless v.s.
Heartless + Vesselless v.s.
WT
Heartless
Vesselless
Heartless + Vesselless
M1 M2 M3 M4
A B C D E F G H

Figure 5

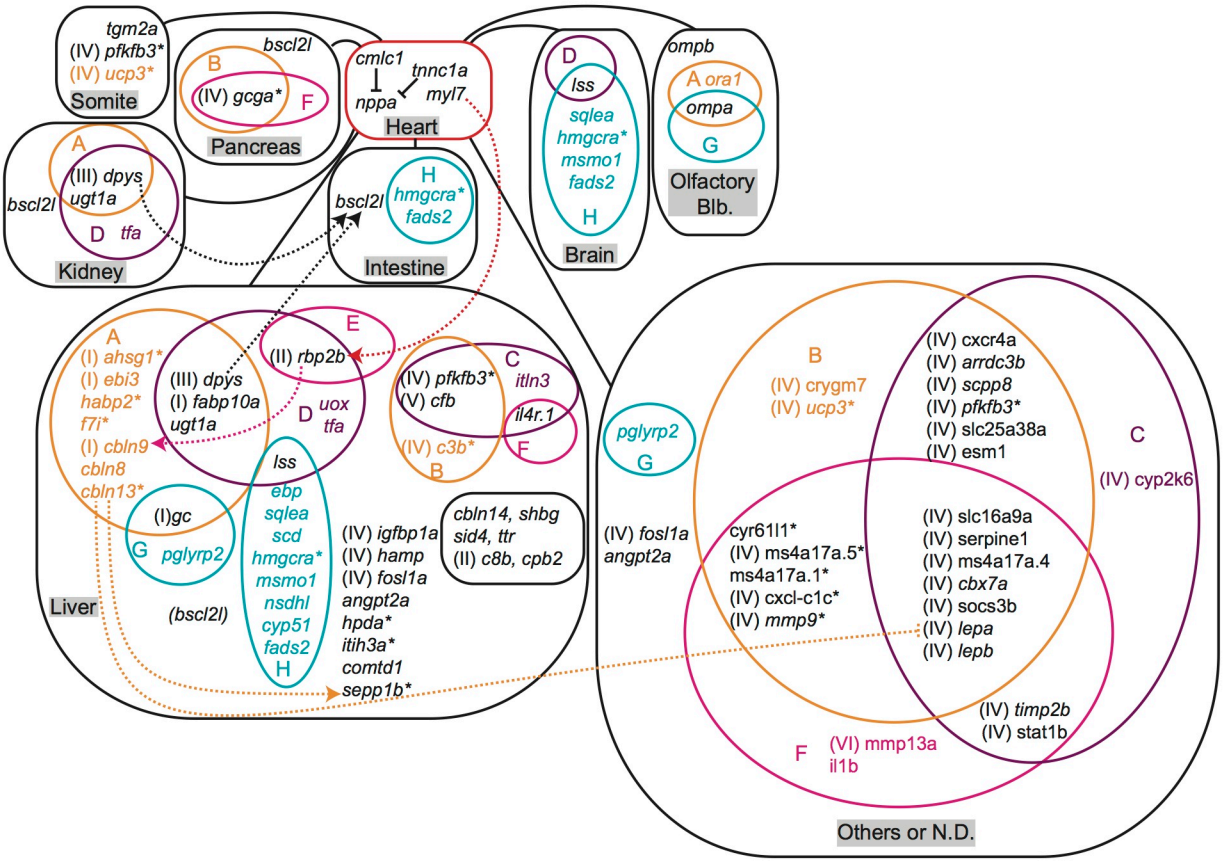
tgm2a
(IV) pfkfb3*
(IV) ucp3*
Somite
bscl2l
B
(IV) gcga*
F
Pancreas
cmlc1
tnnc1a
nppa
myl7.
Heart
D
lss
sqlea
hmgcra*
msmo1
fads2
H
Brain
ompb
A ora1
ompa
G
Olfactory Blb.
A
(III) dpys
ugt1a
bscl2l
D tfa
Kidney
bscl2l
H
hmgcra*
fads2
Intestine
A
(I) ahsg1*
(I) ebi3
habp2*
f7i*
(I) cbln9
cbln8
cbln13*
(I)gc
G pglyrp2
Liver
(bscl2l)
(III) dpys
(I) fabp10a
ugt1a
E
(II) rbp2b
D uox
tfa
lss
ebp
sqlea
scd
hmgcra*
msmo1
nsdhl
cyp51
fads2
H
(IV) pfkfb3*
(V) cfb
C itln3
il4r.1
(IV) c3b*
B
F
(IV) igfbp1a
(IV) hamp
(IV) fosl1a
angpt2a
hpda*
itih3a*
comtd1
sepp1b*
cbln14, shbg
sid4, ttr
(II) c8b, cpb2
pglyrp2
G
(IV) fosl1a
angpt2a
B
(IV) crygm7
(IV) ucp3*
cyr61l1*
(IV) ms4a17a.5*
ms4a17a.1*
(IV) cxcl-c1c*
(IV) mmp9*
(IV) cxcr4a
(IV) arrdc3b
(IV) scpp8
(IV) pfkfb3*
(IV) slc25a38a
(IV) esm1
(IV) slc16a9a
(IV) serpine1
(IV) ms4a17a.4
(IV) cbx7a
(IV) socs3b
(IV) lepa
(IV) lepb
C
(IV) cyp2k6
(IV) timp2b
(IV) stat1b
F
(VI) mmp13a
il1b
Others or N.D.

Figure S1

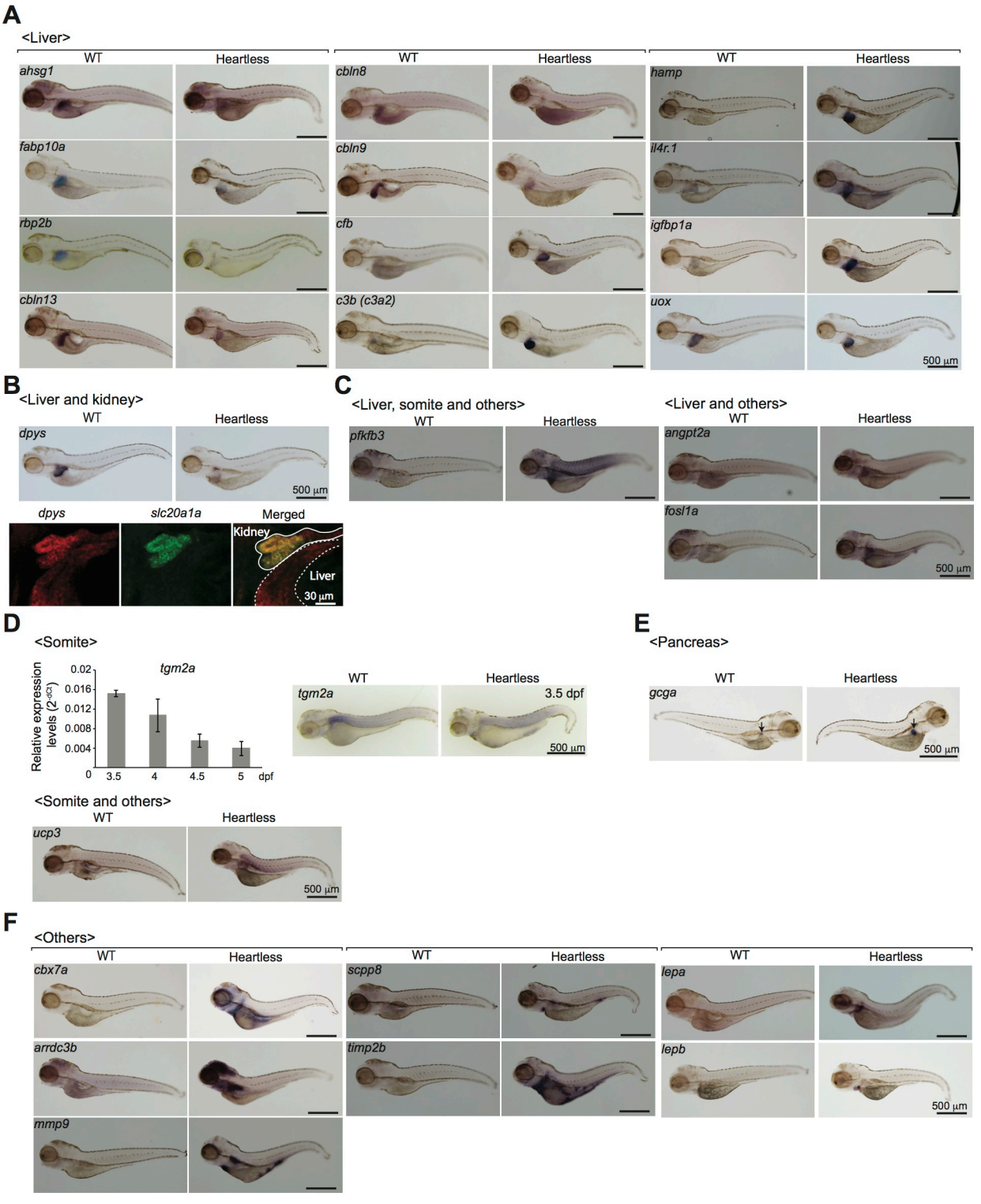
A
<Liver>
WT
Heartless
ahsg1
fabp10a
rbp2b
cbln13
cbln8
cbln9
cfb
c3b (c3a2)
hamp
il4r.1
igfbp1a
uox
500 μm
B
<Liver and kidney>
dpys
500 μm
dpys
slc20a1a
Merged
Kidney
Liver
30 μm
C
<Liver, somite and others>
pfkfb3
<Liver and others>
angpt2a
fosl1a
500 μm
D
<Somite>
tgm2a
Relative expression levels (2-dCt)
0.02
0.016
0.012
0.008
0.004
0
3.5
4
4.5
5
dpf
3.5 dpf
<Somite and others>
ucp3
E
<Pancreas>
gcga
F
<Others>
cbx7a
arrdc3b
mmp9
scpp8
timp2b
lepa
lepb

Figure S2

A

<Liver>

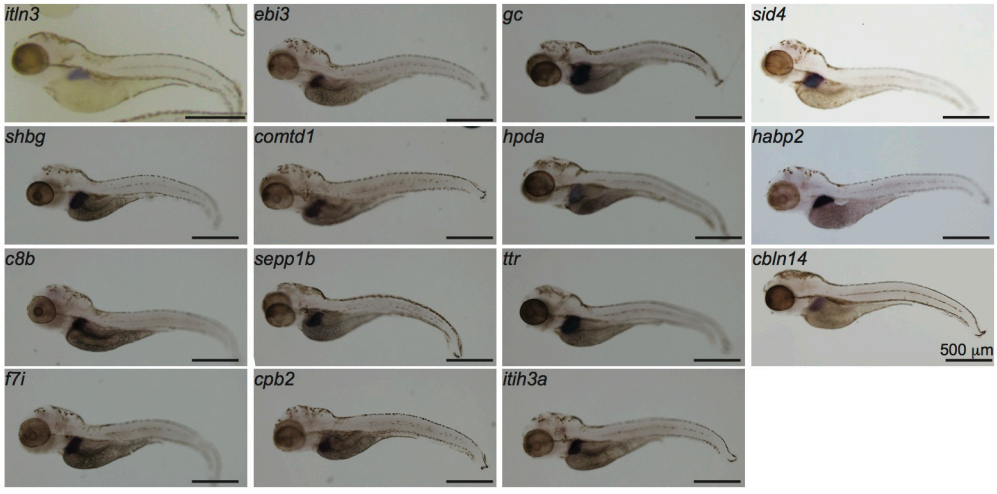

B

<Liver and kidney>

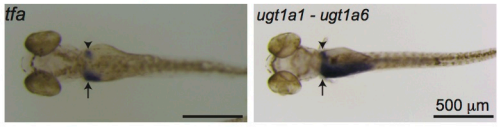

C

<Liver and others>

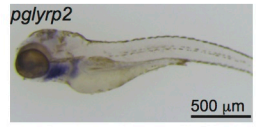

D

<N.D.>

cxcr4a, ms4a17a.5, socs3b, slc25a38a, esm1, cyp2k6, crygm7, slc16a9a
cxcl-c1c, sepine1, ms4a17a.4, stat1b, mmp13a, cyr61l1, ms4a17a.1, il1b

Figure S3

A

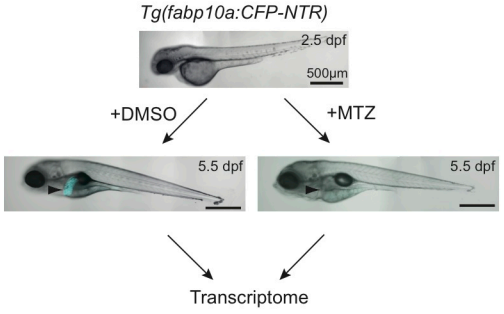
Tg(fabp10a:CFP-NTR)
2.5 dpf
500µm
+DMSO
+MTZ
5.5 dpf
5.5 dpf
Transcriptome

B

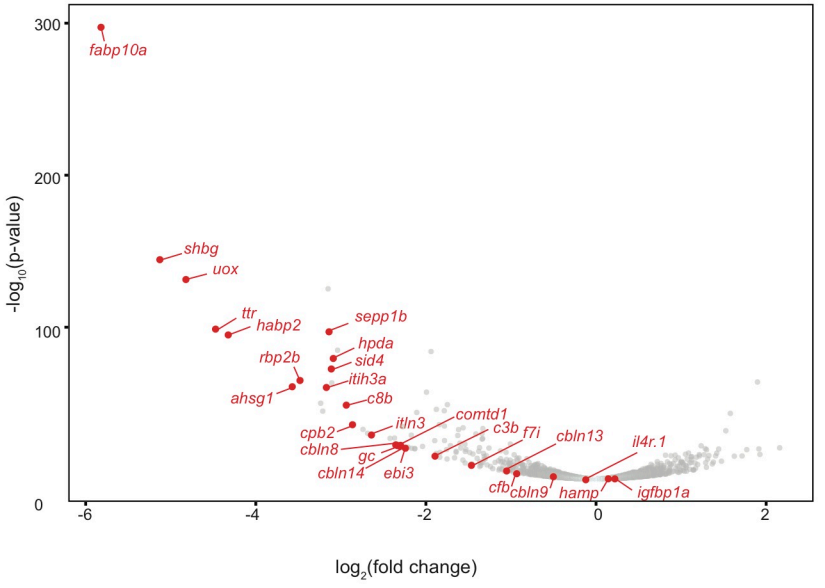
fabp10a
shbg
uox
ttr
habp2
sepp1b
hpda
sid4
rbp2b
itih3a
ahsg1
c8b
cpb2
itln3
comtd1
c3b
f7i
cbln13
il4r.1
cbln8
gc
cbln14
ebi3
cfb
cbln9
hamp
igfbp1a
-log10(p-value)
log2(fold change)
300
200
100
0
-6
-4
-2
0
2

Figure S4

A

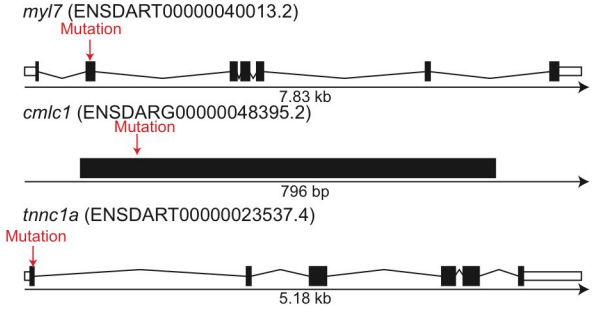

B

```
                          gRNA Target
myl7                GCCAAGAGGGGGAAAACTGCTCAAAGAGGCTC
myl7(+5bp)          GCCAAGAGGGGAAAACTGCTCggcacAAAGA (+5bp)
myl7(+7bp)          GCCAAGAGGGGGAAAACTGCTCttctggaAAA (+7bp)

cmlc1               TTCCAGAGACACCCAAAGAGCCCGAAGTGGACCTGAAAAGCGTCCCGCTG
cmlc1(-16bp)        TTCCAGAc-----------------AAGTGGACCTGAAAAGCGTCCCGCT (-17, +1bp)
cmlc1(+29bp)        AGACACCCAAAGAGCCCGaaaagctctagagactccagagacatccaAAG (+29bp)

tnnc1a              ATGAACGACATCTACAAAGCAGCGgtgagtc
tnnc1a(-5bp)        ATGAACGACATCTA-----CAGCGgtgagtc        (-5bp)
tnnc1a(+13bp)       ATGAACGACATCTACAtcacctacatccacat---CAG (-3, +16bp)
```

C

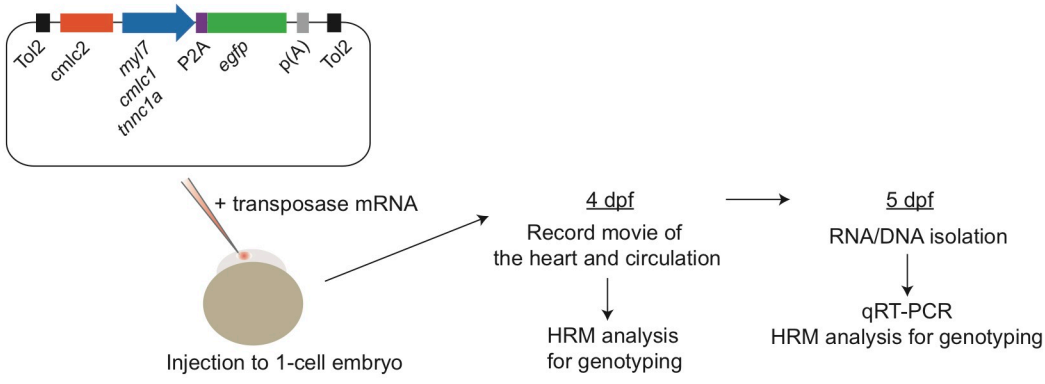

D

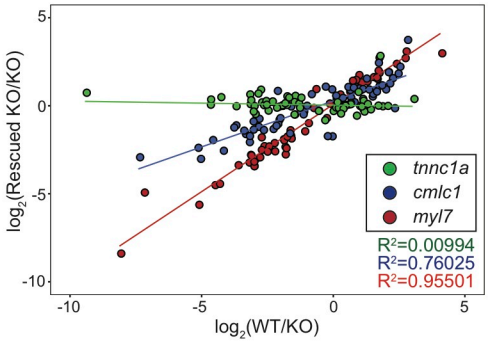

Figure S5

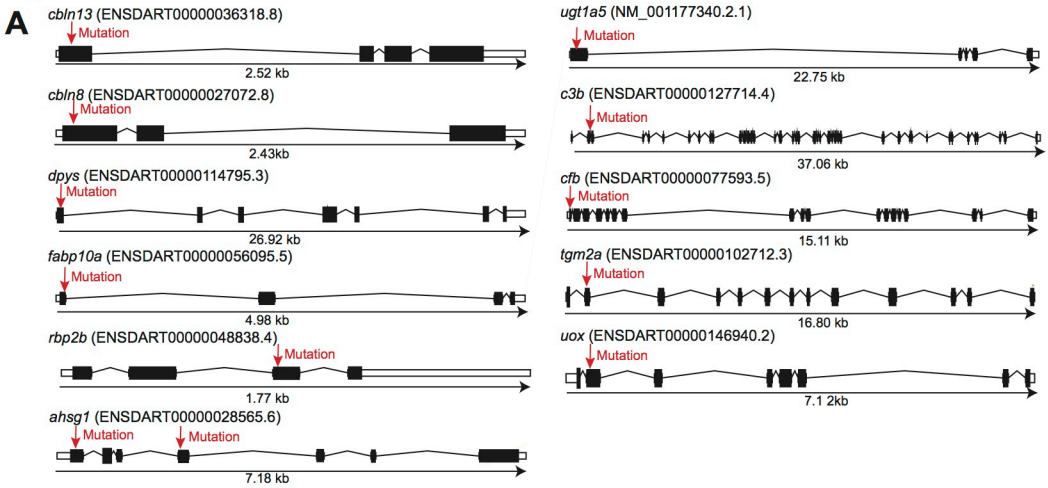
A
cbln13 (ENSDART00000036318.8)
Mutation
2.52 kb
cbln8 (ENSDART00000027072.8)
Mutation
2.43kb
dpys (ENSDART00000114795.3)
Mutation
26.92 kb
fabp10a (ENSDART00000056095.5)
Mutation
4.98 kb
rbp2b (ENSDART00000048838.4)
Mutation
1.77 kb
ahsg1 (ENSDART00000028565.6)
Mutation
Mutation
7.18 kb
ugt1a5 (NM_001177340.2.1)
Mutation
22.75 kb
c3b (ENSDART00000127714.4)
Mutation
37.06 kb
cfb (ENSDART00000077593.5)
Mutation
15.11 kb
tgm2a (ENSDART00000102712.3)
Mutation
16.80 kb
uox (ENSDART00000146940.2)
Mutation
7.1 2kb

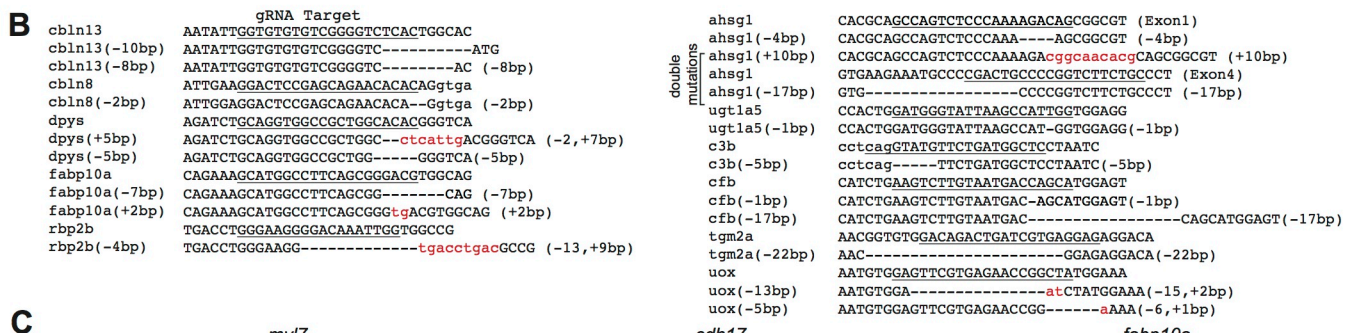
B
gRNA Target
cbln13 AATATTGGTGTGTGTCGGGGTCTCACTGGCAC
cbln13(-10bp) AATATTGGTGTGTGTCGGGGTC----------ATG
cbln13(-8bp) AATATTGGTGTGTGTCGGGGTC--------AC (-8bp)
cbln8 ATTGAAGGACTCCGAGCAGAACACACAGgtga
cbln8(-2bp) ATTGGAGGACTCCGAGCAGAACACA--Ggtga (-2bp)
dpys AGATCTGCAGGTGGCCGCTGGCACACGGGTCA
dpys(+5bp) AGATCTGCAGGTGGCCGCTGGC--ctcattgACGGGTCA (-2,+7bp)
dpys(-5bp) AGATCTGCAGGTGGCCGCTGG-----GGGTCA(-5bp)
fabp10a CAGAAAGCATGGCCTTCAGCGGGACGTGGCAG
fabp10a(-7bp) CAGAAAGCATGGCCTTCAGCGG-------CAG (-7bp)
fabp10a(+2bp) CAGAAAGCATGGCCTTCAGCGGGtgACGTGGCAG (+2bp)
rbp2b TGACCTGGGAAGGGGACAAATTGGTGGCCG
rbp2b(-4bp) TGACCTGGGAAGG----------tgacctgacGCCG (-13,+9bp)
double mutations
ahsg1 CACGCAGCCAGTCTCCCAAAAGACAGCGGCGT (Exon1)
ahsg1(-4bp) CACGCAGCCAGTCTCCCAAA----AGCGGCGT (-4bp)
ahsg1(+10bp) CACGCAGCCAGTCTCCCAAAAGAcggcaacacgCAGCGGCGT (+10bp)
ahsg1 GTGAAGAAATGCCCCGACTGCCCCGGTCTTCTGCCCT (Exon4)
ahsg1(-17bp) GTG----------CCCCGGTCTTCTGCCCT (-17bp)
ugt1a5 CCACTGGATGGGTATTAAGCCATTGGTGGAGG
ugt1a5(-1bp) CCACTGGATGGGTATTAAGCCAT-GGTGGAGG(-1bp)
c3b cctcagGTATGTTCTGATGGCTCCTAATC
c3b(-5bp) cctcag-----TTCTGATGGCTCCTAATC(-5bp)
cfb CATCTGAAGTCTTGTAATGACCAGCATGGAGT
cfb(-1bp) CATCTGAAGTCTTGTAATGAC-AGCATGGAGT(-1bp)
cfb(-17bp) CATCTGAAGTCTTGTAATGAC----------CAGCATGGAGT(-17bp)
tgm2a AACGGTGTGGACAGACTGATCGTGAGGAGAGGACA
tgm2a(-22bp) AAC----------GGAGAGGACA(-22bp)
uox AATGTGGAGTTCGTGAGAACCGGCTATGGAAA
uox(-13bp) AATGTGGA----------atCTATGGAAA(-15,+2bp)
uox(-5bp) AATGTGGAGTTCGTGAGAACCGG------aAAA(-6,+1bp)

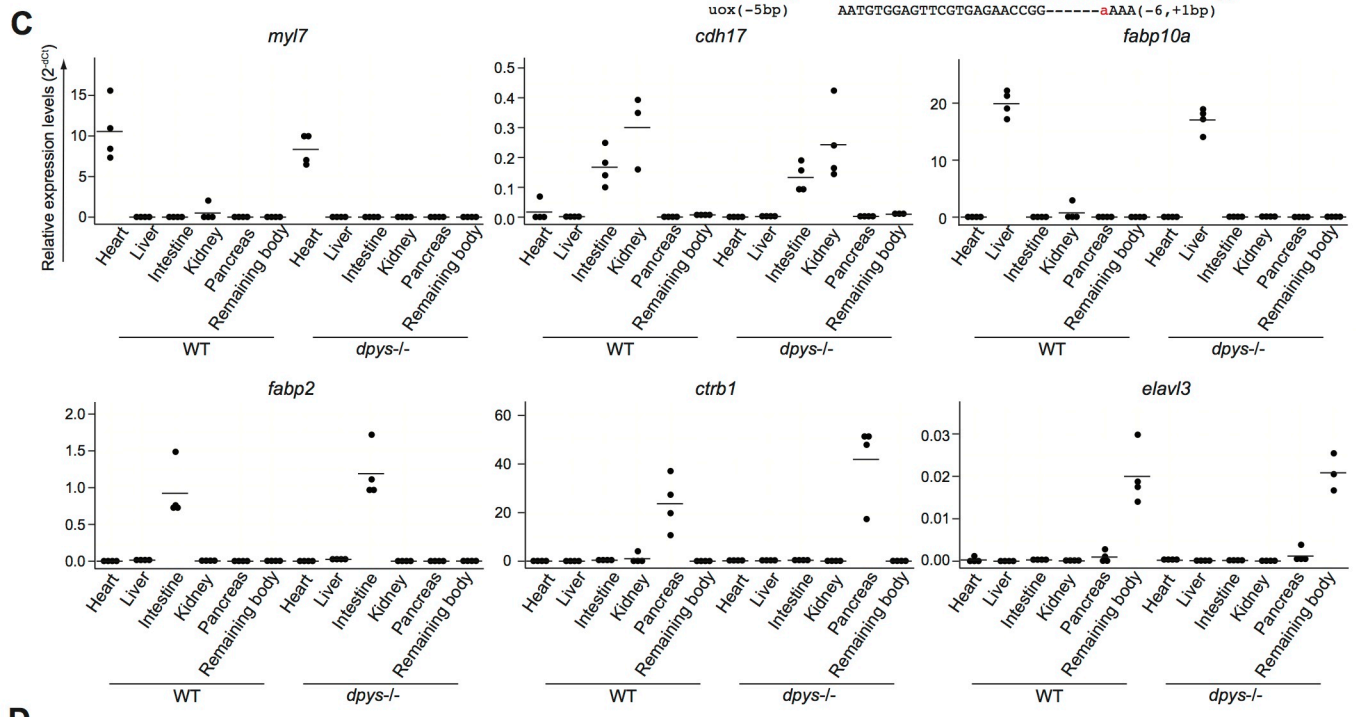
C
myl7
cdh17
fabp10a
fabp2
ctrb1
elavl3
Relative expression levels (2-dCt)
Heart
Liver
Intestine
Kidney
Pancreas
Remaining body
WT
dpys-/-

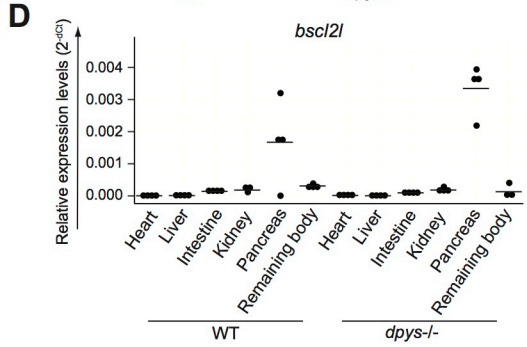
D
bscl2l
Relative expression levels (2-dCt)
Heart
Liver
Intestine
Kidney
Pancreas
Remaining body
WT
dpys-/-

Figure S6

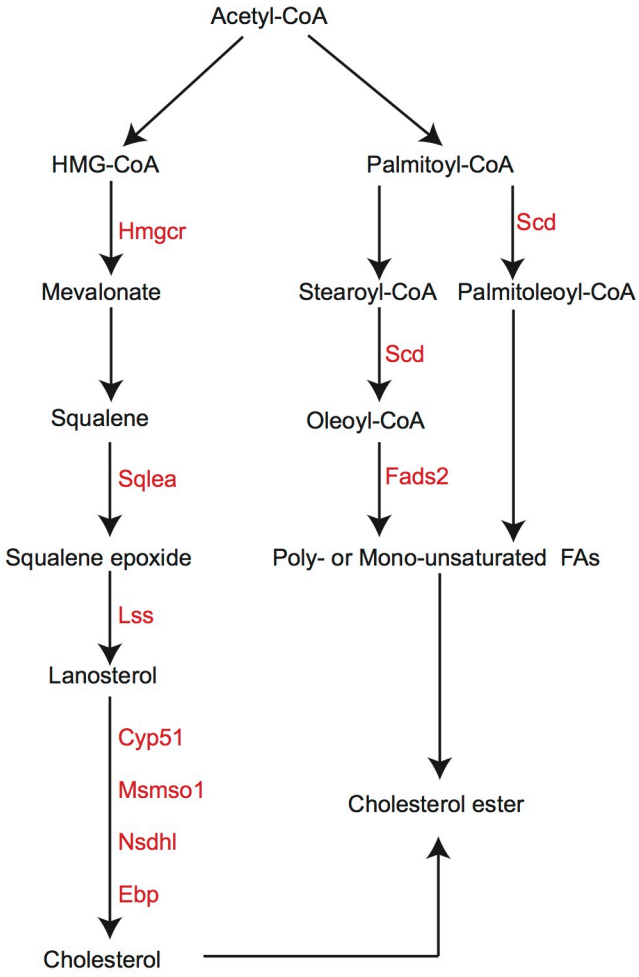
Acetyl-CoA
HMG-CoA
Palmitoyl-CoA
Hmgcr
Scd
Mevalonate
Stearoyl-CoA
Palmitoleoyl-CoA
Scd
Squalene
Oleoyl-CoA
Sqlea
Fads2
Squalene epoxide
Poly- or Mono-unsaturated FAs
Lss
Lanosterol
Cyp51
Msmso1
Nsdhl
Ebp
Cholesterol ester
Cholesterol

Figure S7

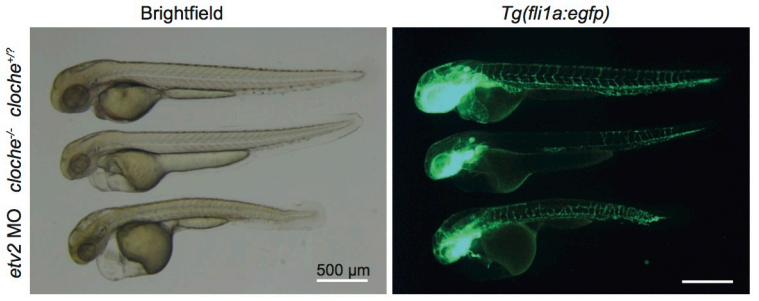

Figure S8

Algorithm 1 Decide gene set A, ..., H in every experimental condition

If blood vessel is ablated
Then {
A: down, B: up,
C: down, D: up,
G: down, H: up.
If cardiomyocyte is ablated
Then E: down, F: up.
Else E: up, F: down.
}
Else {
G: up, H: down.
If cardiomyocyte is ablated
Then {
A: down, B: up,
C: up, D: down,
E: down, F: up.
}
Else {
A: up, B: down,
C: down, D: up,
E: up, F: down.
}
}

Algorithm 2 Decide “up”, “down”, “no-changed” at each fold of gene set expression

Decide up or down gene set A, ..., H in each experimental condition by Algorithm 1:
A_{WT}, $A_{Heartless}$, ..., $H_{Vesselless}$, $H_{Heartless+Vesselless}$
While i in {WT, Heartless, Vesselless, Heartless+Vesselless}
While j in {WT, Heartless, Vesselless, Heartless+Vesselless} do
For X in {A, ..., H} do
If X_i: up and X_j: up then $X_{i\ v.s.\ j}$: no-changed.
Elseif X_i: down and X_j: down then $X_{i\ v.s.\ j}$: no-changed.
Elseif X_i: up and X_j: down then $X_{i\ v.s.\ j}$: down.
Elseif X_i: down and X_j: up then $X_{i\ v.s.\ j}$: up.

Figure S9

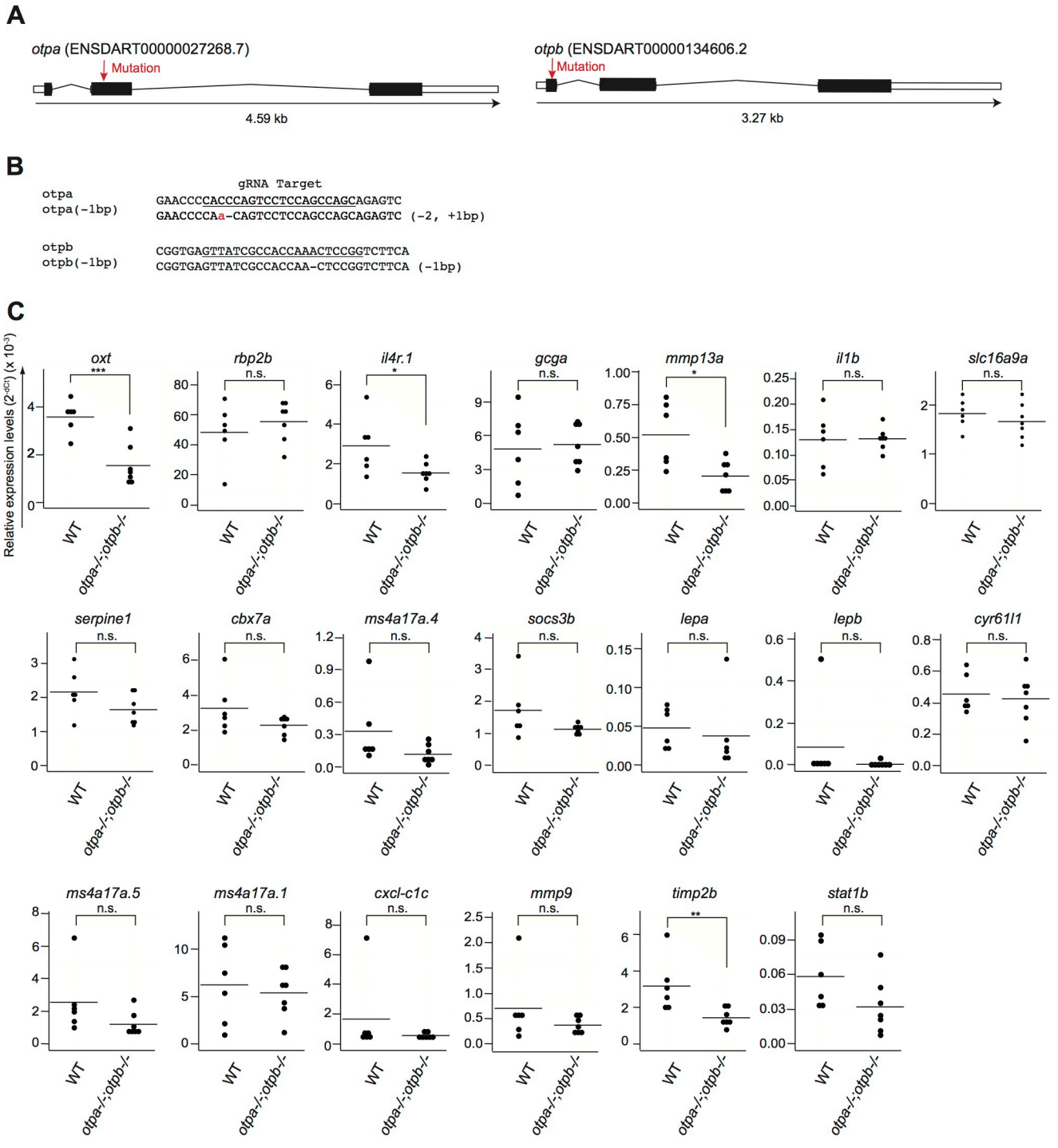
A
otpa (ENSDART00000027268.7)
Mutation
4.59 kb
otpb (ENSDART00000134606.2
Mutation
3.27 kb
B
gRNA Target
otpa
GAACCCCACCCAGTCCTCCAGCCAGCAGAGTC
otpa(-1bp)
GAACCCCAa-CAGTCCTCCAGCCAGCAGAGTC (-2, +1bp)
otpb
CGGTGAGTTATCGCCACCAAACTCCGGTCTTCA
otpb(-1bp)
CGGTGAGTTATCGCCACCAA-CTCCGGTCTTCA (-1bp)
C
Relative expression levels (2-dCt) (x 10-3)
oxt
rbp2b
il4r.1
gcga
mmp13a
il1b
slc16a9a
serpine1
cbx7a
ms4a17a.4
socs3b
lepa
lepb
cyr61l1
ms4a17a.5
ms4a17a.1
cxcl-c1c
mmp9
timp2b
stat1b
n.s.
WT
otpa-/-;otpb-/-

Figure S10

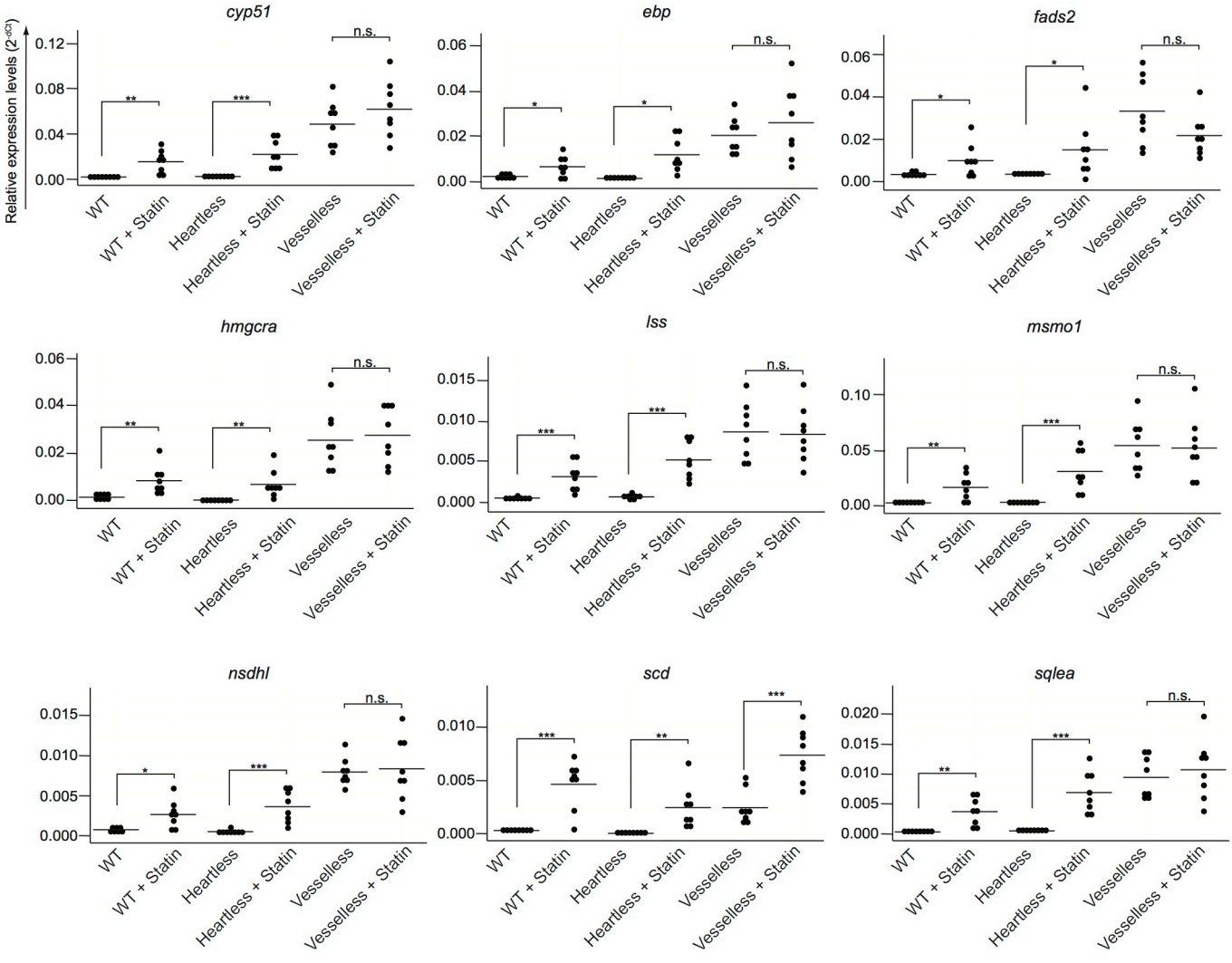
cyp51
ebp
fads2
hmgcra
lss
msmo1
nsdhl
scd
sqlea
Relative expression levels (2-dCt)
WT
WT + Statin
Heartless
Heartless + Statin
Vesselless
Vesselless + Statin
n.s.